

MBBR Nitrification: Investigation of Dissolved Oxygen
Limitation to Enhance Ammonia Removal at Cold
Temperatures

by

Karl I. Todd

A Thesis submitted to the Faculty of Graduate Studies of
The University of Manitoba
in partial fulfilment of the requirements of the degree of

MASTER OF SCIENCE

Department of Civil Engineering
University of Manitoba
Winnipeg

Copyright © 2021 by Karl I. Todd

Abstract

Nitrification remains the most predominant method of ammonia removal wastewater treatment. However, it is well established that seasonal temperature variations have detrimental effects on nitrification which is known to completely cease at temperatures below 5°C in suspended sludge systems. This is of considerable concern to lagoon facilities where nitrification remains unreliable as wastewater temperatures as low as 0.5°C have been observed during winter months. Unlike lagoon facilities, moving bed biofilm reactors (MBBR) technology are capable of achieving significant ammonia removal rates at very cold temperatures (1°C). However, additional methods to enhance nitrification are necessary to meet mandated effluent targets.

In suspended growth systems nitrifier enrichment was determined to be possible through low dissolved oxygen acclimatization which reduces the endogenous decay rate of the nitrifiers thus promoting enrichment. However, there is a lack of knowledge and research as it relates to applying the low DO effect to achieve nitrifier enrichment in biofilms. This research aims to explore enriching nitrifying biofilms under long-term low DO concentrations and study the effects that the enriched biofilms have on nitrification at very low temperatures.

The research concluded that nitrifier enrichment is possible through DO limitation. The study of the reactor performances to temperatures as low as 0.5°C demonstrates a non-linear decline in removal rates between 19.5°C and 0.5°C. When acclimatized to low DO the kinetic threshold temperature was observed at 2.5°C below which, removal rates declined significantly. When acclimatized to high DO the kinetic threshold temperature was observed

at 5°C. The biofilms in the high and low DO reactors showed distinctly different responses to DO. The biofilm mass in low DO reactor was consistently greater than the biofilm mass in the high DO reactor which confirms the hypothesis of the study that long-term low DO is able to inhibit nitrifier endogenous decay and thus result in nitrifier enrichment in the biofilm. In this study, an Arrhenius correction coefficient of 1.150 was found for the transition from 5°C to 0.5°C for the high DO acclimatized MBBR system. A second coefficient of 1.130 was found for the transition from 5°C to 0.5°C in the low DO acclimatized nitrifying MBBR system.

Acknowledgements

I would like to thank my co-advisors Dr. Jan Oleszkiewicz and Dr Tanner Devlin for their knowledge, guidance, support and dedication throughout every stage of my academic career.

I would like to acknowledge and thank Nexom Inc. for supporting this research, without whom this research would not be possible. In particular, I thank Dr Pouria Jabari for being a constant resource throughout this research.

I thank the past and present members of Environmental Engineering research group for their support. In particular, I would like to thank Dr. Wei for his support and expertise during reactor operation and maintenance. I would also like to thank Alessandro di Biase and Daniel Dankewich for always being open to discussion.

I thank Lauren Campbell for being a constant source of encouragement throughout the entirety of the MSc. Program.

Finally, I thank my family who are not sure exactly what I do but are always 100% supportive of my pursuits and are proud of each and every of my accomplishments.

Contents

Abstract.....	2
Acknowledgements	4
List of Figures	7
List of Tables.....	9
1 Chapter 1 – Introduction	1
1.1 Background	1
1.2 Rationale and objectives of the research	4
2 Chapter 2 - Literature Review	5
2.1 Nitrification Process	5
2.2 Nitrification Kinetics	6
2.2.1 Factors Affecting Nitrification.....	8
2.3 Biofilms	15
2.3.1 Bacterial Formation.....	15
2.3.2 Mass Transfer Limitation	16
2.3.3 Biofilm/Biomass Response to Temperature	18
2.3.4 Biomass Cell Viability at Low Temperature	18
2.4 Biofilm Treatment Systems.....	19
2.4.1 Trickling filters.....	20
2.4.2 Rotating biological contact reactors	21
2.4.3 Biological Aerated filtration.....	21
2.4.4 Moving bed biofilm reactors.....	22
3 Chapter 3 - Materials and Methods.....	25
3.1 Reactor configuration.....	25
3.2 Synthetic wastewater	26
3.3 Reactor operation	27
3.3.1 Kinetic batch tests	28
3.4 Analytical methods.....	28
3.4.1 Biofilm Morphology.....	29
3.5 Statistical Analysis	29
4 Chapter 4 - Results	30
4.1 Removal performance	30

4.1.1	Ammonia Removal	30
4.1.2	Nitrite Accumulation	32
4.1.3	Nitrate Production.....	34
4.1.4	pH and Alkalinity	35
5	Chapter 5 - Discussion.....	39
5.1	Low Temperature Effect on Nitrification.....	39
5.1.1	Nitrification Recovery at 0.5°C.....	41
5.2	Temperature Correction Coefficient Analysis.....	42
5.2.1	Effect of DO Limitation on the Temperature Correction Coefficient.....	45
5.3	DO Limitation on Nitrification.....	47
5.4	Biofilm response.....	50
5.5	Nitrification Batch Kinetics.....	52
6	Engineering Significance	55
7	Summary and Conclusion.....	56
8	References.....	59

List of Figures

Figure 2-1 - Visual representation of the metabolism of aerobic autotrophic bacteria – AOB, NOB (Adapted from Metcalf and Eddy 2014)	6
Figure 2-2 - Idealized representation of the mass transfer of solutes from the bulk liquid through the biofilm (Adapted from Metcalf and Eddy, 2014).....	16
Figure 3-1 Schematic of laboratory setup.	25
Figure 4-1 - Ammonia removal efficiencies in R1 and R2 at temperatures from 19.5°C to 0.5°C	31
Figure 4-2 - Ammonia removal efficiencies in R1 and R2 against dissolved oxygen.	31
Figure 4-3 - Nitrite concentrations in R1 and R2 at temperatures from 19.5°C to 0.5°C.....	33
Figure 4-4 - Nitrite concentration in R1 and R2 against dissolved oxygen.....	33
Figure 4-5 - Nitrate concentrations in R1 and R2 at temperatures from 19.5°C to 0.5°C.....	34
Figure 4-6 - Nitrate concentration in R1 and R2 against dissolved oxygen.....	35
Figure 4-7 - Time-course measurements of Influent and effluent alkalinity against temperature and dissolved oxygen for R1 (A), time-course measurements of Influent and effluent pH for R1(B).	37
Figure 4-8 - Time-course measurements of Influent and effluent alkalinity against temperature and dissolved oxygen for R2 (A), time-course measurements of Influent and effluent pH for R2(B).	38
Figure 5-1- Recovery in ammonia oxidation in R1 and R2 at 0.5 degrees Celsius.	42

Figure 5-2 - Comparison between the effluent ammonia and nitrate predicted by the BioWin model and the experimental effluent ammonia and nitrate for the transition from 5°C to 0.5°C in R1 using a temperature correction factor of 1.15.....	43
Figure 5-3 - Comparison of the ammonia removal rates predicted with Delatolla et al. (2009) model and observed experimental ammonia removal rates in R1.....	45
Figure 5-4 - Comparison between the effluent ammonia and nitrate predicted by BioWin model and experimental effluent ammonia and nitrate for the transition from 5°C to 0.5°C in R2 using a temperature correction factor of 1.13.	46
Figure 5-5 - Comparison of the ammonia removal rates predicted with Delatolla et al. (2009) model and observed experimental ammonia removal rates in R2.....	47
Figure 5-6 - Changes in the nitrifying biofilm mass in R1 and R2 at 19.5°C, 12.5°C, 10°C and 0.5°C.....	51
Figure 5-7 - Biofilm thickness in R1 and R2 at 19.5°C, 12.5°C, 10°C and 0.5°C.....	52
Figure 5-8 - Biomass-specific removal rates determined from the kinetic batch tests for R1 and R2 at 19.5°C, 12.5°C, 10°C and 0.5°C.	54
Figure 5-9 - Surface area-specific removal rates determined from the Kinetic batch tests for R1 and R2 at 19.5°C, 12.5°C, 10°C and 0.5°C.	54

List of Tables

Table 2-1 maximum specific growth rate (μ_{max}), nitrogen half velocity constant, Oxygen half velocity constants and biomass yields of AOB, NOB and heterotrophs in wastewater[3,19]. . 7	
Table 2-2 The effect of organic loading rates on the nitrification rates in MBBR systems [24]	14
Table 3-1 Operational parameters for R1 and R1 through the experiment.....	26
Table 3-2 Feed characteristics for influent fed to the MBBR systems.	27

1 Chapter 1 – Introduction

1.1 Background

Nutrient-rich wastewater streams are deleterious in aquatic environments and have been identified as significant contributors to surface water toxicity and eutrophication. As a result, nutrient removal is strictly regulated by the Canadian Wastewater Systems Effluent Regulations Fisheries Act (WSER). The WSER regulates the discharge of four deleterious substances: carbonaceous biochemical oxygen demanding matter (cBOD), suspended solids (TSS), total residual chlorine and un-ionized ammonia [1]. With respect to un-ionized ammonia, WSER mandates effluent discharges contain less than 1.25 mg-N/L un-ionized ammonia at 15 ± 1 °C. Un-ionized ammonia has the potential to cause acute toxicity in fish species at relatively low concentrations of 0.1 to 10 mg L⁻¹. As such, WSER also mandates that effluent discharges pass an acute lethality test (LC50), defined as less than 50% mortality of rainbow trout after 96 hours in 100% effluent. Studies have reported failure of the LC50 test at total ammonia concentrations between 11 mg/L to 48 mg/L [2].

The removal of ammonia in wastewater is most commonly achieved through biological nitrification [3]. However, conventional biological treatment processes such as suspended growth systems, while capable of reducing cBOD and TSS have been demonstrated to be impeded at temperatures below 10°C and near non-existent below 5°C [4,5]. Hence, there are significant challenges in achieving mandated effluent limits in the rural and northern regions of Canada, the United States, and Europe that utilize lagoons as the predominant method of

wastewater treatment where wastewater temperatures as low as 0.5°C have been observed in the winter months.

Several studies on suspended growth systems have investigated methods to improve cold temperature nitrification through nitrifier enrichment. One such strategy is increasing the solids retention time (SRT) to compensate for the low growth rates at cold temperatures. However, increased SRT in suspended sludge systems results in high sludge concentration, high sludge loading on clarifiers, and filamentous growth. Another strategy utilizes nitrifier bioaugmentation while maintaining short SRT, which has been shown to improve nitrification rates below 10°C [6–8]. However, this process requires high dosage of an external source of nitrifiers. Another promising strategy for nitrifier enrichment in suspended sludge is through inhibiting the nitrifier endogenous decay rate by acclimatizing the bacteria to low dissolved oxygen (DO) [9]. However, an increase in the SRT may be necessary to compensate for lower kinetic rates due to low DO.

In contrast with suspended sludge systems, nitrifying biofilm technologies, which have inherently long SRTs, present a unique solution for the negative effects of long SRT in suspended sludge and have proven to provide some compensation for the temperature sensitivity of nitrifiers. Thus, biofilm technologies would be particularly effective in treating post-carbon removal effluent from the last lagoon in a multi-lagoon treatment system where effluent temperatures as low as 0.5°C are common during winters.

While several attached growth technologies have been investigated for their applicability at cold temperatures, the overall simplicity, efficiency, and many inherent advantages of

attached growth systems make moving bed biofilm reactor (MBBR) technology an ideal biofilm technology for post-carbon removal low temperature nitrification. At the lab and pilot scale, several studies have explored MBBR technology as an add-on to multi-lagoon treatment systems to treat wastewater at 1°C [10–13]. At the lab scale, Hoang et al. (2014) observed removal rates at 1°C to be 17% of the rate at 20°C operation, Almomani et al. (2014) using real wastewater achieved ammonia removal rates at 1°C to be 42% of the rate observed at 20°C and Ahmed et al. (2019) observed removal efficiencies greater than 55% [10,14,15]. At the pilot scale, Young et al. (2017) demonstrated removal efficiencies at 1°C to be greater than 70% at loading rates below 250 gNm⁻³d⁻¹. All studies have operated at DO levels greater than 7 mg/L [12]. These results demonstrate the ability of MBBR technology to achieve significant ammonia removal at very low temperatures. However, meeting federal effluent ammonia limits requires additional methods to compensate for the lower kinetics.

As previously mentioned, studies have investigated the effect of low DO on the nitrifier population in suspended sludge and have found that long-term low DO will inhibit nitrifier decay, which results in the relative increase in the biomass nitrifier concentration [9,16]. However, there is a lack of knowledge and research as it relates to applying the low DO effect to achieve nitrifier enrichment in biofilms. Hence, this study aims to explore enriching nitrifying biofilms under long-term low DO operation and study the effects that the enriched biofilms have on nitrification at 0.5°C.

1.2 Rationale and objectives of the research

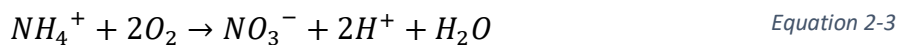
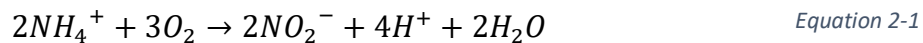
The aim of this research is to investigate the effect of long-term low dissolved oxygen concentrations on nitrifying biofilms. The study includes exploring the nitrification kinetics at temperatures as low as 0.5°C as well as the biofilm response to temperature and DO. This research will provide new knowledge on the performance of MBBR technology as it applies post-carbon removal nitrification at very cold temperatures. Additionally, the study will provide useful information on process control at very cold temperatures. The specific objectives of this research are as follows:

- I. The ammonia removal rate at 0.5°C in nitrifying MBBR systems acclimatized to high and low DO.
- II. The kinetic threshold temperature below which MBBR ammonia removal kinetics is significantly impacted.
- III. The Arrhenius temperature correction coefficients for nitrifying biofilms acclimatized to low and high DO while exposed to temperatures as low as 0.5°C.
- IV. The mass and thickness response of nitrifying biofilms acclimatized high and low DO and exposed to temperatures down to 0.5°C.

2 Chapter 2 - Literature Review

2.1 Nitrification Process

Biological nitrification is the predominant method of ammonia removal from wastewater streams. Nitrification is performed by autotrophic bacteria, which use CO₂ as a carbon source and oxidize inorganic nitrogen to obtain energy [3]. Two groups of autotrophic bacteria are primarily responsible for nitrification, Ammonia oxidizing bacteria (AOB) and Nitrite Oxidizing Bacteria (NOB), each responsible for a specific phase of the nitrification process. AOB primarily consists of Nitrosomonas, Nitrosococcus, Nitrospira, Nitrocystis, and Nitrosogloea, which are capable of oxidizing ammonia into nitrite. NOB consists primarily of Nitrobacter and Nitrocystis, which oxidize nitrite to nitrate [9]. Stoichiometric relationships of the two-step process are:



As shown in the above stoichiometric relationships, alkalinity and oxygen are consumed in the nitrification process. Oxygen requirements for nitritation and nitratation steps of the reaction are 3.43 g-O₂/g-NH₄⁺-N and 1.14 g-O₂/g-NO₂⁻-N, respectively. Therefore, the total required oxygen for complete nitrification is 4.57 g-O₂/g-NH₄⁺-N. Alkalinity is consumed through the production of hydrogen ions. 7.14 g-CaCO₃/g-NH₄⁺-N during the oxidation of ammonia to nitrate [3]. Nitrifying

bacteria also need CO₂ and phosphorus for cell growth. However, with such low cell yields, the CO₂ in air is typically adequate [3]. Nitrosomonas and Nitrobacter are also able to utilize small amounts of exogenous organic material as a carbon source [17]. Biomass synthesis also contributes to ammonia removal by consuming small amounts of the total ammonia. Ammonia consumption for biomass synthesis has been reported to be less than 2% of the total ammonia removed by nitrifiers during nitrification [18].

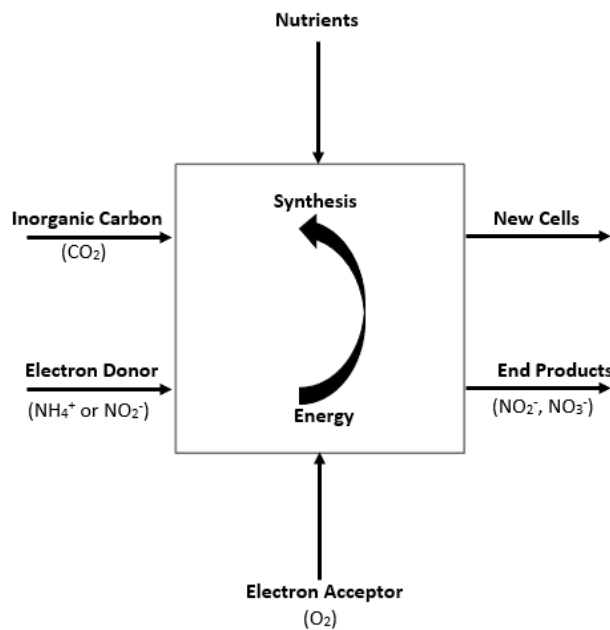


Figure 2-1 - Visual representation of the metabolism of aerobic autotrophic bacteria – AOB, NOB (Adapted from Metcalf and Eddy 2014)

2.2 Nitrification Kinetics

The Monod growth kinetics model is the most widely accepted mathematical model use for in describing NH₄-N and NO₂-N oxidation kinetics [3]. It describes the microbial growth rates of AOB and NOB as a function of the nitrogen species being oxidized, dissolved oxygen (DO) concentration and the endogenous decay rate [1]:

$$\mu = \mu_{max} \left(\frac{S_N}{S_N + K_N} \right) \left(\frac{DO}{DO + K_0} \right) - b_N$$

Where: $\mu_{N,max}$ is the maximum specific growth rate of nitrifiers (d^{-1}), S_N is the concentration of nitrogen specie being oxidized (g/m^3), K_N is the nitrogen-specie half-velocity constant (g/m^3), b_N is the nitrifier specific endogenous decay rate (d^{-1}), DO is the dissolved oxygen concentration (g/m^3), and K_0 is the oxygen saturation constant (g/m^3).

A transformed Monod equation was established to calculate steady-state substrate removal rate in pure nitrifier culture system [3].

$$r_N = \left(\frac{\mu_{max}}{Y_n} \right) \left(\frac{S_N}{S_N + K_N} \right) \left(\frac{DO}{DO + K_{0,N}} \right) X_n$$

Where: r_N = substrate removal rate ($mgL^{-1}d^{-1}$), X_n is concentration of active biomass (mg/L), Y_n is the true yield for cell synthesis ($mg \text{ cell}/mg \text{ substrate}$), DO is the dissolved oxygen concentration (g/m^3), and K_0 is the oxygen saturation constant (g/m^3). X_n is the concentration of the active biomass which conduct the synthesis process and the Y_n quantifies the substrate removal rate by a specific amount of biomass.

Table 2-1 maximum specific growth rate (μ_{max}), nitrogen half velocity constant, Oxygen half velocity constants and biomass yields of AOB, NOB and heterotrophs in wastewater[3,19].

	μ_{max} (1/d)	K_N (g/m^3)	K_0 (g/m^3)	Y(g-cells/g-substrate-utilized)
AOB	0.33 - 2.2	0.14 - 5.6	0.3 - 1.3	0.04 - 0.13
NOB	0.28 - 1.8	0.05 - 8.4	0.25 - 1.7	0.02 - 0.08
Heterotrophs	7 - 17	8 - 12	0.0007 – 0.1	0.37 - 0.79

When comparing AOB and NOB to heterotrophic bacteria, the AOB and NOB are at a clear competitive disadvantage (Table 2-1). The high oxygen half-velocity constant in AOB and NOB indicate that significantly more oxygen is required to remove ammonia and nitrite as opposed organic carbon. Nitrifiers have much lower yields than heterotrophs as nitrifiers are less efficient at producing and using energy. The doubling time of nitrifiers can range from 8 - 60 hours, while just approximately 30 minutes for heterotrophs [3]. This generation time of nitrifiers has been reported to increase to as much as 200 h at 5°C [20].

2.2.1 Factors Affecting Nitrification

2.2.1.1 Effect of pH

Nitrification rates are highly sensitive to pH. Optimum overall nitrification rates occur between pH values 7.5 – 8 and decline significantly outside of this range. AOB accomplishes optimum ammonia oxidation between pH 7.0 - 8.0, while NOB perform efficient nitrate oxidation in the pH range of 7.2 - 8.2 [3,21]. Free ammonia, NH_3 , and nitrous acid, HNO_2 , have been shown to inhibit both AOB and NOB activity. The high sensitivity of AOB and NOB activity to pH can be explained by the dependence of free ammonia and nitrous acid on pH. The concentration of free ammonia is dependent on the total ammonia concentration ($\text{NH}_4\text{-N} + \text{NH}_3\text{-N}$) as well as the pH and temperature in the reactor. The HNO_2 concentration is dependent on pH, temperature and NO_2 concentration. At higher pH and temperature, the NH_3 fraction of the total ammonia concentration increases, while at lower pH and temperatures, a greater fraction of the NO_2 shifts to HNO_2 [3]. The $\text{NH}_3\text{-N}$ and HNO_2 are estimated by Equation 2-4 and Equation 2-5:

$$NH_3 = \frac{TAN(10^{pH})}{\left(\frac{1}{K_a}\right) + 10^{pH}} \quad \text{Equation 2-4}$$

$$HNO_2 = \frac{NO_2}{(K_n)(10^{pH})} \quad \text{Equation 2-5}$$

Where TAN = total NH₃-N + NH₄-N concentration (g/m³), K_a = the ionization constant for ammonia at temperature T°C, NO₂ = nitrite concentration and K_n = the ionization constant for nitrous acid at temperature T°C.

The required alkalinity for nitrification is 7.14 g-CaCO₃/g-NH₄-N oxidized [3]. Therefore, in activated sludge treatment systems receiving wastewaters with low alkalinity or high ammonia concentrations alkalinity must be added to maintain operational alkalinity of 50 – 60 mg/L as CaCO₃ [3].

2.2.1.2 Effect of Temperature

Studies have shown that nitrifying bacteria in biological treatment systems are extremely sensitive to low temperatures. Nitrification rates in suspended sludge have been reported to decrease as much as 91% at temperatures below 5°C compared to the rates at 20°C [5]. Nitrifying bacteria are as mesophilic, as such, the optimum temperature for nitrification is between 28°C – 36°C with a thermal death point for AOB between 54°C – 58°C [19]. Little to no growth of Nitrosomonas or Nitrobacter occurs below 4°C. The inhibitory effect of cold temperature is greater on Nitrobacter than Nitrosomonas [22]. Therefore, it is not uncommon for nitrite ions to accumulate during cold temperatures.

The impact of temperature on the maximum growth is often described by Arrhenius equation (Equation 2-6) in which a temperature correction coefficient, θ , is applied.

$$\mu_{max,T} = \mu_{max,20} * \theta^{(T-20)} \quad \text{Equation 2-6}$$

Where maximum specific growth rate at any temperature ($\mu_{max,T}$) is related to the maximum specific growth rate at 20°C ($\mu_{max,20}$) and the Arrhenius temperature correction coefficient (θ) [3,23].

Previous studies on suspended sludge have reported a large range of θ values between 1.028 to 1.165 [5]. A coefficient of 1.072 has been widely accepted for the design of suspended growth wastewater treatment systems [3,24]. However, there are factors such a temperature shock and acclimatization period that influence the temperature correction coefficient [25]. Hwang and Oleszkiewicz (2007) were able to demonstrate a clear difference in the temperature correction coefficient in suspended sludge when the temperature was gradually decreased from 20°C to 10°C as opposed to an immediate decrease in temperature over the same temperature range. The gradual decrease was adequately predicted by the correction coefficient 1.072 while the sudden change had a higher correction coefficient of 1.116. It should be noted that nitrification rates returned to the expected range to be after an acclimatization period [25]. Several studies on attached growth systems have demonstrated similar distinctions between the temperature correction coefficient due to gradual temperature decrease and immediate temperature decrease [15,26]. The studies have also shown the dependence of the temperature correction coefficient on the acclimatization

period. In Delatolla et al. (2009), the dependence of the temperature correction coefficient on the exposure time at 4°C in BAF systems was described by Equation 2-7 [26]:

$$\theta = 3.81 * 10^{-2} * \ln(t) + 9.83 * 10^{-1} \quad \text{Equation 2-7}$$

Several studies have applied the Delatolla et al model to simulate the transition from 4°C to 1°C in MBBR systems with differing levels of success [11,15,27]. Young et al. (2017) and Hoang et al. (2014) found strong correlation for the transition from 4°C to 1°C. While Ahmed et al. (2019) found poor correlation [15]. Thus, Ahmed et al. (2019) proposed a modified Delatolla et al. Theta model (Equation 2-8) to predict the temperature correction coefficients for MBBR systems as a function of exposure time below 4°C [15]:

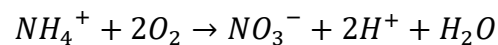
$$\theta = 1.17 * 10^{-1} * \ln(t) + 9.19 * 10^{-1} \quad \text{Equation 2-8}$$

Few studies exist which study the rapid reduction of temperature in MBBR systems. However, these studies have all demonstrated significant adverse impacts on nitrification when subjected to cold-shock as opposed to gradual reduction in temperature [15,28]. In a study by Delatolla et al. (2010) conducted between 14°C and 4°C, the abrupt temperature change resulted in the ammonia removal rate reducing significantly followed by a gradual recovery in the ammonia removal rate after 3 days [28]. Ahmed et al. (2019) compared the performance of a cold shocked nitrifying MBBR system from 10°C and 1°C to a similar system gradually acclimatized to 1°C. The results of the study showed ammonia removal rates in the shocked reactor to be on average 21% lower than the rates in the reactor that was slowly acclimatized.

Moreover, ammonia removal rates never recovered which contrasts with the study by Delatolla et al. (2010) between 14°C and 4°C [15].

2.2.1.3 Effect of Dissolved oxygen

Oxygen is a major limiting factor in nitrification. The theoretical oxygen requirements per the nitrification stoichiometric equations are: 3.43 mg-O₂/mg-NH₄-N and 1.14 mg-O₂/mg-NO₂-N [3].



Unlike ammonia which can exist as free ammonia (NH₃-N) and can be present in sufficient concentrations to inhibit nitrification, dissolved oxygen (DO) has limited solubility in water and will not inhibit nitrification when provided in excess [3]. Studies in suspended sludge have shown that the growth rate of AOB increase very little at a DO concentration above 2 mg/L. However, NOB are more sensitive to DO and showed a reduced growth rate at a DO concentration less than 4 mg/L [29]. As such, partial nitrification has been observed at low DO concentrations [3]. Nitrification has been reported to cease entirely below a DO concentration of 0.2 mg/L [30]. DO mass transfer limitations in suspended sludge affect nitrification rates as nitrifiers are distributed within activated sludge flocs that contain heterotrophic bacteria and other solids, therefore nitrification deep within the floc is limited by access to DO [3].

Limited oxygen conditions in biofilms can be significantly different than in suspended sludge systems, as oxygen availability for biofilms are subjected to diffusion limits. Zhu and Chen. (2002) determined that maintain sufficient DO more important in the biofilm process than in

the suspended growth processes due to the nature of diffusion limitations through the biofilm matrix [31]. Zhang et al. (1995) studied the DO concentration profiles within biofilms and reported diffusion resistance in throughout the biofilm matrix which caused the DO concentration to fall rapidly within the biofilm and was the limiting factor as it was below 2 mg/L within the biofilm even though the bulk solution had a sufficiently high DO concentration [32]. The study also noted the presence of heterotrophs in the same order of magnitude as nitrifiers in the biofilm's bottom layer, which likely increased oxygen consumption and contributed to the rapid depletion of DO in the biofilm.

Several studies have explored the long-term effect of low DO concentration on nitrification [33–35]. The study carried out by Hanaki et al. (1990) determined that the ammonia oxidation rate per unit biomass of ammonia oxidizers was reduced due to low DO levels. However, the growth yield of the ammonia oxidizers was elevated by low DO, which increased the concentration of ammonia oxidizers in the reactor, thereby compensating for the effects of low DO. On the other hand, the study reported that nitrite oxidizers have no such system of compensation, resulting in significant reductions in the nitrite oxidation rate [33]. A more recent study by Liu and Wang. (2013) contradicts the study by Hanaki et al. (1990) showing that nitrite oxidation at low DO can be improved after long acclimatization to low DO [34]. Additionally, the study argued that the enrichment of both AOB and NOB was likely a result of the inhibition of the nitrifier endogenous decay due to low DO rather than an increase in the growth yield as argued by Hanaki et al [34]. Munz et al. (2011) demonstrated a near-linear

relationship between oxygen concentration and the endogenous decay rate for DO between 0 - 7 mg/L, which supports the findings by Lui and Wang. (2013) [36].

2.2.1.4 Effect of organic Loading

Extensive research has been conducted on the effect of organic loading on the nitrification process and have found that the efficiency of nitrification is affected by the organic loadings. The most critical impacts of excess organics on nitrification are the contribution to additional oxygen demand and the competition with nitrifying bacteria for oxygen [31,37,38]. Fast-growing heterotrophic bacteria which utilize organic carbon as their energy source will outcompete slow-growing nitrifying bacteria for oxygen [39]. Studies have shown that the proportion of nitrifiers in a microbial population decreases with increasing carbon to nitrogen (C/N) ratio [40].

In biofilms, the ideal conditions for nitrifying bacteria growth occur when the Carbon/Nitrogen (C/N) ratio is between 0 and 1 [24]. When the Carbon/Nitrogen ratio is greater than 1, heterotrophic bacteria can form in the outer layer of the biofilm and outcompete the nitrifiers for solutes such as oxygen and nutrients. Very little oxygen will be available for nitrifiers until the carbon has been depleted. Thus, low carbon environments are ideal for nitrifier growth. On the other hand, heterotrophs are beneficial to maintaining nitrifiers in the biofilm structure through extracellular polymeric substances (EPS) secretion, which protects the nitrifying bacteria against detachment [41].

Table 2-2 The effect of organic loading rates on the nitrification rates in MBBR systems [24]

Organic Loading (g-BOD₅/m²·d)	Nitrification Rate (gNH₄-N/m²·d)
--	---

1 - 2	0.7-1.2
2 - 3	0.3-0.8
>5	0

2.3 Biofilms

2.3.1 Bacterial Formation

Biofilms can comprise of microbial species and that form on a range of biotic and abiotic surfaces [42]. Biofilm formation is generally understood to be a multistep process. In the first stage of biofilm formation, a conditioning layer is formed on the surface of the medium, which forms the foundation on which the biofilm grows. This layer modifies the surface charge, potential and tensions favourably to facilitate accessibility to bacteria [43]. The next stage is reversible adhesion; bacteria move from bulk solution to the conditioned surface by physical forces and bacterial appendages. At this stage, adhesion is reversible and will be reversed if the repulsive forces exceed the attractive forces [39,41,42]. Following this stage, irreversible adhesion occurs where reversibly adsorbed cells consolidate their adhesion to the surface by excreting extracellular polymeric substances (EPS) and become irreversibly adsorbed. Following irreversible adhesion, there is an exponential growth phase where cells divide, resulting in daughter cells spreading outwards to form a mushroom-like structure [46]. The exponential growth phase depends heavily on physical and chemical (pH, temperature, dissolved oxygen, and nutrient availability and source) environment [43]. The final stages of biofilm development are maturation and detachment. In the maturation phase, there is

stationary growth where the rate of biofilm growth is equivalent to the rate of biofilm decay [47].

2.3.2 Mass Transfer Limitation

Solute transport through biofilms is governed by diffusion principles through the biofilm matrix. Solutes (oxygen, nutrients) are transported to a stagnant liquid layer near the surface of the biofilm known as the mass transfer boundary layer (MTBL). The MTBL does not allow advective transport, as such, solutes diffuse through the MTBL into the biofilm matrix. This rate of diffusion across the MTBL into the biofilm is termed the substrate surface flux and is defined by Equation 2-9 and Equation 2-10 [3].

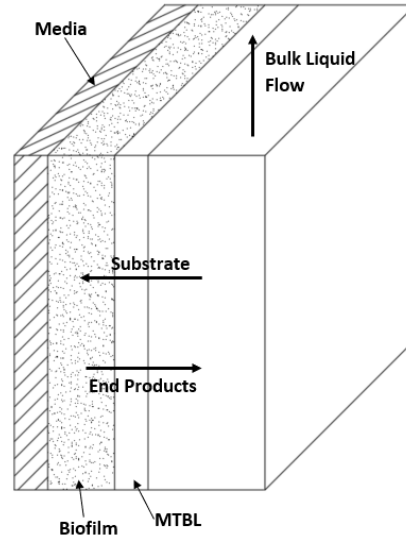


Figure 2-2 - Idealized representation of the mass transfer of solutes from the bulk liquid through the biofilm (Adapted from Metcalf and Eddy, 2014).

$$r_{sf} = -D_w \left(\frac{S_b - S_s}{L} \right) \quad \text{Equation 2-9}$$

$$r_{bf} = -D_e \frac{dS}{dx} \quad \text{Equation 2-10}$$

Where r_{sf} is the rate of substrate surface flux ($\text{g}/\text{m}^2 \cdot \text{d}$), D_w is the diffusion coefficient of substrate in water (m^2/d), S_b is the bulk liquid substrate concentration (g/m^3), S_s is the substrate concentration at outer layer of biofilm (g/m^3) and L is the effective length of stagnant film (m), r_{bf} is the rate of substrate flux in the biofilm due to mass transfer ($\text{g}/\text{m}^2 \cdot \text{d}$), D_e effective diffusivity coefficient in the biofilm (m^2/d) and dS/dx is the substrate concentration gradient ($\text{g}/\text{m}^3 \cdot \text{m}$). The rate of diffusion into the biofilm is typically slower than the bacterial metabolism rate which results in different chemical environments that vary at various depths in biofilm, which in turn creates different microbial communities throughout the biofilm [3].

The electron donor and electron acceptor concentrations (oxygen or nitrate) has important implications on the diffusion process. Williamson and McCarty. (1976) proposed a model to determine if a surface flux limitation exists. That method is described by Equation 2-11. The proposed method can also be used to determine the relative electron acceptor bulk liquid substrate concentrations needed to sustain electron donor utilization within the biofilm. Nitrification rates in biofilm systems are often dissolved oxygen limited [45].

$$S_{ba} < \frac{D_{wd} v_a m v_a}{D_{wa} v_d m v_d} S_{bd} \quad \text{Equation 2-11}$$

2.3.3 Biofilm/Biomass Response to Temperature

Previous studies have investigated the impacts of low temperatures on nitrifying biofilms in MBBR systems at temperatures as low as 1°C. Hoang et al. (2014) observed an increase of approximately 31% in the biofilm thickness from 20°C to 1°C [48]. Young et al. (2017) observed an increase in the biofilm mass and thickness from 20°C to 1°C. The mass increased 70% while the biofilm thickness increased 75% [27]. Ahmed and Delatolla (2021) observed an increase of 25% in the biofilm thickness between 10 °C and 4 °C, followed by smaller increases of 7% and 10% at 2°C and 1°C [49]. In the above-mentioned studies, the increase in the biofilm thickness was attributed to the lower metabolic rate in the biofilm which allowed for increased substrate availability throughout the biofilm, and thus promote biofilm growth, particularly of filamentous bacteria and carbohydrate producers associated with increases in biofilm thickness [27,48,49]. However, studies of the endogenous decay rate for nitrification, b_N , demonstrate dependence on temperature, which would suggest that as temperatures decreases the lower endogenous decay rate will result in greater net biomass growth resulting in thicker biofilms. Studies in suspended sludge have reported the endogenous decay rate to double with a 10°C increase in temperature [50]. However, the endogenous decay is generally accepted as following an Arrhenius-type temperature relationship with a correction factor 1.029 typically used for design above 10°C [3].

2.3.4 Biomass Cell Viability at Low Temperature

Several studies have investigated the cell viability in nitrifying MBBR biofilms at temperatures ranging from 20°C – 1°C and have observed an increase in the cell viability at cold

temperatures [27,48,49]. Hoang et al. (2014) did not observe a significant change in biofilm cell viability between 20°C and 1°C. However, a significant increase in cell viability after four months at 1°C was observed [48]. Young et al. (2017) observed an increase in the cell viability at 1°C relative to 20°C. There was 26% increase in the live cell fraction of the total cells in the biofilm [27]. Ahmed and Delatolla (2021) observed 32% increases in cell viability at 1°C as opposed to 10°C [49]. These studies have attributed the increase in the cell viability at cold temperatures to an increase in substrate availability throughout the biofilms [27,48,49].

2.4 Biofilm Treatment Systems

Biofilm treatments systems are biological systems that utilize microorganisms that are attached and colonized on some type of inert support medium to perform carbon oxidation and nitrification. In attached growth systems, the medium can be either fixed or suspended in the reactor. Biomass attachment provides protection from external predation and toxic compounds in aquatic environments, thereby providing a competitive advantage over the suspended sludge systems [51]. Additionally, compared with conventional suspended sludge systems, attached growth systems perform efficient carbon removal and nitrification under harsh conditions such as higher organic loading rates (OLR), low pH, and cold temperatures due to more effective biomass retention in the reaction zone resulting in higher cellular retention times and lower activation energy required by the immobilized microorganisms [52,53]. Several attached growth technologies have been implemented successfully to perform carbon removal and nitrification; they include: rotating biological contactor,

biological aerated filtration (BAF), trickling filters, and moving-bed biofilm reactors (MBBR) [54–57].

Trickling filters and rotating biological contactors have proven capable of achieving nitrification and carbon removal efficiencies between 85 – 90% at various loading conditions and under conventional treatment temperatures [3,54]. However, new systems such as MBBRs and BAFs are more efficient than RBCs and trickling filters having reported removal efficiencies greater than 90% under harsher environmental conditions [48,58]. Additionally, systems such as MBBR and BAF have the advantage of smaller space requirements and are popular in communities where small footprints are required [59].

2.4.1 Trickling filters

Trickling filters are biofiltration technology made up of a vessels containing inert media which supports microbiological growth to remove carbon and performs nitrification [60]. The bacteria in trickling filters rely on natural air flow for oxygen unlike activated sludge systems, which rely on some form mechanical aeration. Trickling filters use rocks or engineered plastic packing as the support media for the biofilm [61]. Wastewater is distributed over the top of the media and trickles downwards as a thin film across the surface of the packing, where oxygen, soluble organics and nutrients diffuse through biofilm [62]. Several studies have investigated the temperature dependence of nitrification in biofilters. Zhu and Chen. (2002) observe no significant effects of temperature on trickling filter performance between 14 - 27°C [31]. Saidu (2009) observed similar result with there being no statistical differences in

ammonia removal rates between 13°C and 20°C [63]. Wortman and Wheaton. (1991) observed a linear effect of temperature on biofiltration performance between 7- 35°C [64].

2.4.2 Rotating biological contact reactors

Rotating biological contactor (RBC) are fairly efficient biofilm technologies used to treat wastewater. A biofilm is established on the surface of the media, which metabolizes the organic materials and nutrients contained in the wastewater as the RBC rotates and absorbs oxygen from the air [65]. Rotation also provides turbulence which enables the removal any excess biomass which is then removed through the conventional clarification process. The RBC system has the advantage of relatively small space requirements, simple process control and monitoring, resistance to shock and toxic loads, low operating and maintenance cost, less sludge production and high biomass concentration per volume reactor [65]. However, optimization and adaptability of RBC under different environmental conditions is a challenge that RBC technology faces. For low temperature applications, RBC systems used in municipal treatment plants have been proven capable of achieving significant nitrification rates at an average temperature of 13°C [56]. At temperatures below 13°C, a significant decline in nitrification rates has been observed. RBC systems are estimated to experience performance losses of 4.5%/°C [66].

2.4.3 Biological Aerated filtration

Biological aerated filters (BAFs) are high rate attached growth wastewater treatment systems that are capable of providing carbon removal and nitrification and denitrification. BAF contains inert media that provides a large surface area per unit volume for biofilm

development [3]. The media is submerged in the reactor allowing the reactor to act as a submerged filter that filters suspended solids. The process allows for the elimination of the secondary clarification, allowing the system to operate independently of the sludge settling parameters that limit the design and operation of conventional activated sludge treatment systems [67]. BAF systems can be operated in up-flow or downflow configurations. In the downflow configuration, air is supplied in contact with the final effluent for a greater period of time which is important when simultaneous carbon removal and nitrification is required [55]. However, the up-flow configuration is preferred as the downflow configuration traps rising air resulting in undesirable head loss, increased clogging, resulting in increased backwashing frequency [3]. BAF processes have several advantages over conventional activated sludge processes; these include small space requirements, the ability to effectively treat dilute wastewaters and no issues with sludge settling characteristics [3,55]. On the other hand, the process requires a more complex operation, maintenance and higher capital cost[3]. Delatolla et al. (2009) demonstrated that this technology is capable of performing significant amounts of nitrification at temperatures as low as 4°C [68]. The effective exposure time to low temperatures was a key finding in the study and of crucial importance to nitrification. The Delatolla et al. Theta model is characterized by Equation 2-8 in which the temperature correction coefficient increases with the exposure time to 4°C.

2.4.4 Moving bed biofilm reactors

Moving Bed Biofilm Reactors (MBBR) are attached growth systems that utilize carriers to facilitate biofilm development. In MBBRs, the carriers are maintained in suspension and are

allowed to move freely within the bulk liquid [57]. MBBR technology can be configured to perform carbon removal, nitrification and denitrification. A wide variety of carriers exist to be used in MBBR; however, most installations use plastic biocarriers [3]. The available protected surface area for biofilm growth varies based on the manufacturer of the carriers and typically range $189 \text{ m}^2/\text{m}^3 - 5500 \text{ m}^2/\text{m}^3$ [69]. An important design factor for MBBR systems is the filling fraction, which is the ratio of the volume of carriers to the total volume of the reactor [3]. The filling fraction affects the performance and the volumetric capacity of the reactor; as such, a filling fraction that achieves performance requirements while allowing for adequate mixing and reactor hydrodynamics should be selected [69]. The maximum filling fraction should not exceed 70%, beyond which mixing becomes challenging [3,70].

MBBR processes have several advantages over conventional activated sludge(CAS), such as small space requirements, simplicity of operation with no need for SRT control and sludge recycle, low operation and maintenance cost in comparison to CAS and other attached growth treatment systems and the elimination of concerns of sludge bulking in the secondary clarifiers and its effects on operation and effluent quality [3]. Like other attached systems, MBBR systems have greater resistance to pH shock, shock loads, temperature variations, and toxic compounds [69].

2.4.4.1 Application of MBBR Technology at Low Temperatures

The ability of MBBR systems to achieve nitrification at cold temperatures has been well demonstrated. Andreatolla et al. (2000) observed ammonia removal efficiencies of 73% at 8°C despite a COD loading $1.3\text{--}11.8 \text{ g COD m}^{-2}\text{d}^{-1}$ [71]. Several studies have explored MBBR

systems as a post-carbon removal technology for lagoon facilities to achieve nitrification at very low temperatures (1°C). Almomani et al. (2014) using real wastewater achieved ammonia removal rates at 1°C to be 42% of the rate observed at 20°C [10]. Hoang et al. (2014) observed removal rates at 1°C to be 17% of the rate at 20°C operation. To model the measured results, Hoang et al. (2014) applied the Delatolla et al. (2010) transition model (Equation 2-7) and found strong correlation ($R^2 = 0.86$) during the acclimatization period [48]. Young et al. (2017) demonstrated removal rates at 1°C to be greater than 70% of the rates at 20°C for loading rates below $250 \text{ gNm}^{-3}\text{d}^{-1}$. In the study by Young et al. (2017), a temperature correction coefficient of 1.09 was applied for the temperature reduction from 12°C to 7.4°C which allowed for adequate modelling of the experimental results ($R^2 = 0.89$). However, between 5°C to 1°C, and the first 10 days at 1°C the removal rates were well predicted by the Delatolla et al. (2010) model (Equation 2-7) with $\theta = 1.125$ at the initial 1°C time point ($R^2 = 0.77$) [12]. A subsequent study by Ahmed et al (2020) between 10°C - 1°C contrasts with the study by Young et al. (2017). Ahmed et al. (2020) determined removal rates at 1°C to be 40% lower than the rate reported in Young et al. (2017) [12,15]. Additionally, a temperature correction coefficient of 1.049 was used to predict with strong correlation ($R^2 = 0.93$) the ammonia removal rates between 10°C and 4°C. A second of 1.149 was able to predict with strong correlation the rates at 1°C. The discrepancy between the studies was attributed to the limited temperature control in the Young et al. (2017) study which benefited from temperature fluctuations [15].

3 Chapter 3 - Materials and Methods

3.1 Reactor configuration

Two bench-scale reactors, namely reactor 1 (R1) and reactor 2 (R2) were operated under continuous conditions using temperature-controlled fridges to house the reactors during periods of the study below room temperature. BioPorts 600-14 media (Nexom; Winnipeg, MB) having a protected surface area of $589 \text{ m}^2/\text{m}^3$ was chosen for the study. The operating volumes in both reactors were 16 Litres with a carrier fill fraction of 25% by volume. The total available surface area for biomass colonization was 2.4 m^2 in each reactor. Fine bubble diffusers were used to provide air, while mechanical mixing was implemented in both reactors to ensure adequate mixing and suspension of the carriers. Figure 3-1 shows a schematic of the laboratory setup. A summary of the operational parameters is shown in Table 3-1.

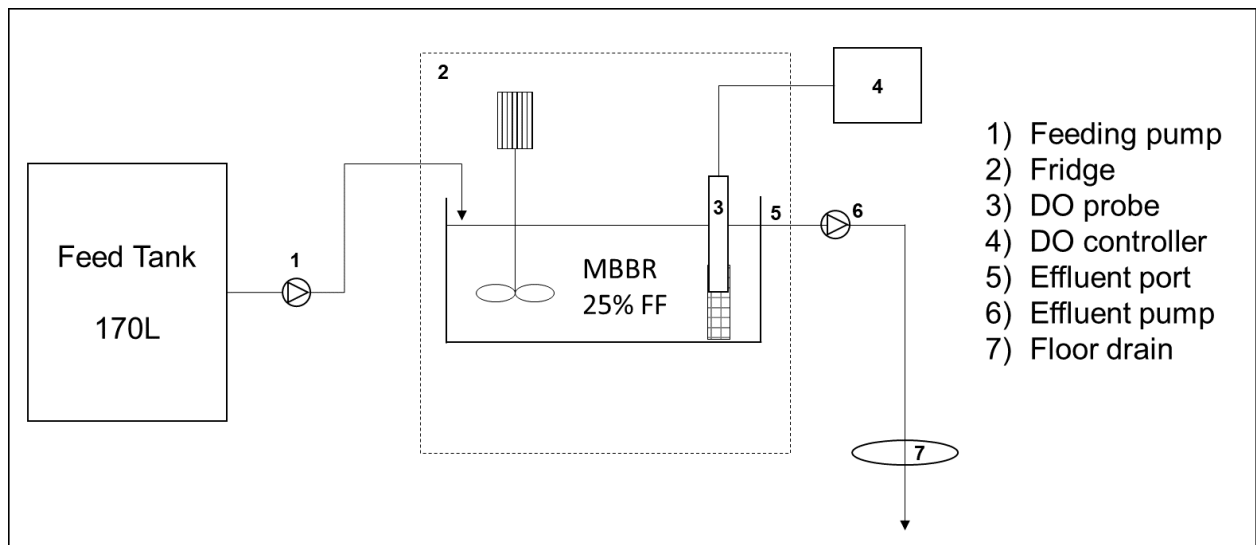


Figure 3-1 Schematic of laboratory setup.

Table 3-1 Operational parameters for R1 and R1 through the experiment.

Parameter	Operating Parameters		Unit
	R1	R2	
Flow	24.25	24.25	L d ⁻¹
Volume	16	16	L
Fill Fraction (FF)	25	25	%
Bioportz plastic carriers	589	589	m ² m ⁻³
HRT	0.66	0.66	d
NLR	45.97 ± 4.08	45.82 ± 2.69	g-NH ₄ -N m ⁻³ d ⁻¹
Available surface area	2.4	2.4	m ²
SALR	0.31 ± 0.02	0.31 ± 0.02	g-NH ₄ -N m ⁻² d ⁻¹
Media volume	8	8	L

3.2 Synthetic wastewater

Low carbon synthetic wastewater was used for the entirety the study to provide stable ammonia loading rates with limited variations. The synthetic wastewater was prepared according to the following recipe: NH₄CL (30 mg NH₄/L), NaHCO₃ (214 mg/L), KH₂PO₄ (2 mg-P/L), yeast (10 mg-COD/L) (Table 3-2). The yeast was supplied at a concentration of 10 mg COD/L to imitate the readily degradable carbonaceous content of wastewater leaving the final pond in a multi-pond lagoon system. Trace elements were provided to prevent nutrient-limitation [72]. Thus, the micronutrients content of the synthetic wastewater was: 1.5 mg L⁻¹ of FeCl₂·4H₂O; 0.0845 mg L⁻¹ MnSO₄·H₂O; 0.18 CaCl₂; 0.69 mg L⁻¹ MgSO₄·H₂O; 0.476 mg L⁻¹ CoCl₂·6H₂O; 0.0061 mg L⁻¹ H₃BO₃; 0.14 mg L⁻¹ ZnSO₄·7H₂O; 0.0025 mg L⁻¹ CuSO₄·5H₂O; 0.556 mg L⁻¹ Na₂MoO₄·2H₂O; 2.38 mg L⁻¹ NiCl₂·6H₂O; and 0.263 mg L⁻¹ Na₂SeO₃·5H₂O [69]. The Influent constituents were dissolved in 170 L of tap water.

Table 3-2 Feed characteristics for influent fed to the MBBR systems.

Constituent	Concentration (mg/L)	
	R1	R2
Ammonia (NH ₄ ⁺)	30.41 ± 2.04	30.31 ± 1.78
Nitrite (NO ₂ ⁻ -N)	0.84 ± 0.93	1.07 ± 1.11
Nitrate (NO ₃ ⁻ -N)	1.33 ± 0.67	1.35 ± 0.67
COD as yeast	10	10
Alkalinity	267.64 ± 12.52	261.58 ± 15.85
pH	7.64 ± 0.18	7.62 ± 0.18

3.3 Reactor operation

Reactors 1 and 2 were seeded with waste activated sludge from the West End Water Pollution Control Centre (Winnipeg, Manitoba). After seeding, the reactors were operated for 24 days (37 HRT cycles) at 19.3°C ± 0.4°C and 19.2°C ± 0.4°C, respectively until steady-state was achieved. During this phase, the DO concentrations in the reactors were maintained at 6.1 ± 0.3 mg/L and 6.1 ± 0.1 mg/L. Upon achieving steady-state, nitrogen purging was introduced into R2 to reduce and maintain the DO concentration at 2.1 ± 0.3 mg/L. R2 was then operated at a DO concentration of 2.1 ± 0.3 mg/L for a 36-day acclimatization period during which the DO in R1 was maintained at 6.1 ± 0.3 mg/L. Following the acclimatization period, the temperatures in R1 and R2 were reduced to 10°C in 2.5°C increments over 31 days and operated at 10°C for 14 days, during which steady-state was achieved. The temperatures in the reactors were then reduced to 0.5°C in 2.5°C increments over 27 days. The temperature reduction below 10°C was accompanied by a step-wise DO increase to 6 mg/L in R2. R1 was maintained above 6 mg/L. The reactors were operated at 0.5°C for 161 days. Nexom Inc. has

measured similar full-scale temperature profiles as far spread as Glencoe Ontario, Lorette Manitoba, and Dawson Creek British Columbia.

3.3.1 Kinetic batch tests

Kinetic batch tests were performed to quantify the biomass-specific removal rates and surface area-specific removal rates. The reactors were operated to steady state at 19.5°C, 12.5°C, 10°C, 5°C, and 0.5°C, after which 36 carriers were removed in triplicates from each reactor and transferred to 1 L beakers. The beakers were then filled to the 1 L mark with the synthetic wastewater described in section 3.2. Marina 50 air pumps were used to supply air and provide mixing through fine bubble ceramic diffusers. Each kinetic batch test was conducted over a 5-hour period with samples extracted hourly and analyzed for NH_4^+ , NO_2^- -N, NO_3^- -N concentrations.

3.4 Analytical methods

Samples were analyzed to determine the NH_4^+ -N, NO_2^- -N, NO_3^- -N concentrations, as well as temperature, pH, and alkalinity. The reactors were operated at constant flow rates and with consistent influent concentrations, as such grab samples were collected from each reactor three times a week on average. QuickChem flow injection analyzer (Lachat QuikChem 8500, HACH, CA) was used to analyze the nitrogen constituents while electrodes were used to monitor but not control the pH in the reactors (pH 6, Oakton, USA). Alkalinity was measured according to Standard Methods [73]. IQ SensorNet probes were used to continuously monitor, record, and control the DO and temperature in the reactors.

3.4.1 Biofilm Morphology

To quantify the biofilm mass, three carriers taken in triplicates (9 total) were harvested from each reactor. The carriers were then thoroughly abraded with a brush and flushed with de-ionized water to remove the biofilm. The flushed liquid was analyzed for TSS and VSS using standard methods [73]. Microscopic analysis and biofilm thickness measurements were done using SteREO Discovery (Zeiss, DE).

3.5 Statistical Analysis

The student t-test was used to determine statistical significance for differences in the nitrogen concentrations, ammonia removal rates and ammonia removal efficiencies with a p-value less than 0.05 indicating significance, p-value between 0.05 and 0.1 indicates marginal significance and p-value of 0.1, and greater indicating insignificance. The coefficient of determination (R^2) was used to evaluate the quality of fit of the modeled and measured results with R^2 greater than 0.70 considered a good fit.

4 Chapter 4 - Results

4.1 Removal performance

4.1.1 Ammonia Removal

Ammonia removal efficiencies in R1 and R2 reached 98% at room temperature before step-wise temperature reduction began. The ammonia removal efficiency remained above 98% until the temperature reached 5°C, at which point the ammonia removal efficiency in R1 fell to an average of $87.7 \pm 7\%$, while the removal efficiency in R2 remained at $98.1 \pm 0.5\%$. When the temperature in the reactors reached 2.5°C, the ammonia removal efficiency in R1 was observed to be $45.8 \pm 4.8\%$, while the removal efficiency in R2 fell to an average of $65.4 \pm 4\%$. The ammonia removal efficiency in both reactors fluctuated widely at the beginning of operation at 0.5°C. In R1, the removal efficiencies fluctuated between 1% and 31% over the first 56 days. The performance then stabilized at $10 \pm 1.1\%$ over the next 34 days, followed by a gradual improvement in the removal efficiency to 34% at the end of operation at 0.5°C. In R2, removal efficiencies fluctuated between 9% and 31% over the first 28 days. Performance in R2 then stabilized at $12 \pm 3.7\%$ over the next 30 days, followed by a gradual increase in the removal efficiency to 26% towards the end of operation at 0.5°C (Figure 4-1 and Figure 4-2).

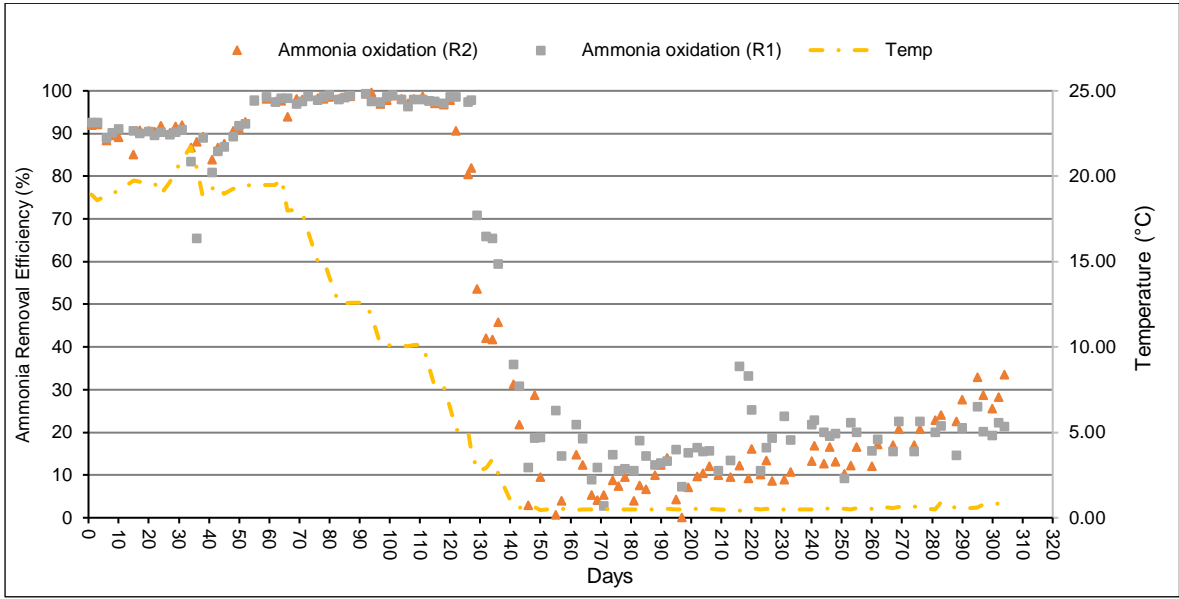


Figure 4-1 - Ammonia removal efficiencies in R1 and R2 at temperatures from 19.5°C to 0.5°C

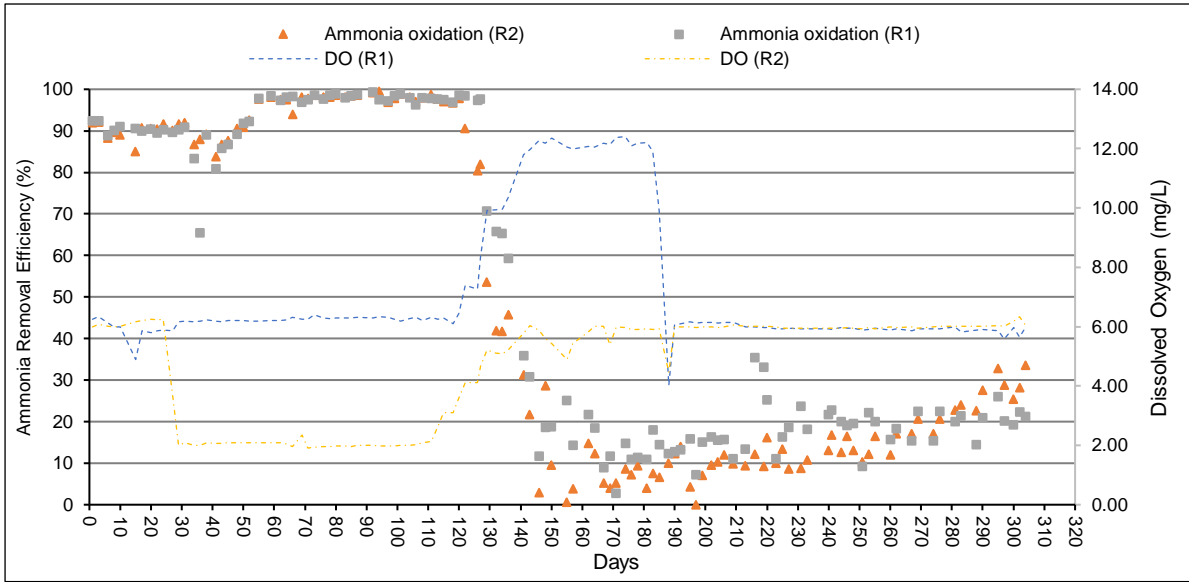


Figure 4-2 - Ammonia removal efficiencies in R1 and R2 against dissolved oxygen.

4.1.2 Nitrite Accumulation

Nitrite accumulation in the reactors appeared to be a function of temperature rather than DO. Upon reaching steady state at room temperature, the nitrite concentration in R1 remained low at 0.29 ± 0.19 mg/L until the temperature in the reactor reached 4.65 ± 0.46 °C upon which the nitrite concentration spiked to 2.70 mg/L. The increase in nitrite at 4.65 ± 0.46 °C corresponded with an approximate 20% decrease in ammonia removal efficiency. After a 7-day period, the nitrite concentration decreased to 0.22 ± 0.24 mg/L and remained at such for 56 days before once again accumulating to 1.59 mg/L followed by a gradual reduction to 0.15 mg/L towards the end of operation at 0.5°C (Figure 4-3).

The nitrite concentration in R2 was 0.16 ± 0.11 mg/L between room temperature and 4.78 ± 0.54 °C. Upon reaching 4.78 ± 0.54 °C the nitrite concentration increased to 2.03 mg/L over a 10-day period, after which it decreased to 0.51 ± 0.31 mg/L. Similar to R1, nitrite accumulation occurred once again after 28 days of operation at 0.5°C followed by a gradual reduction to 0.12 mg/L at the end of operation at 0.5°C (Figure 4-4).

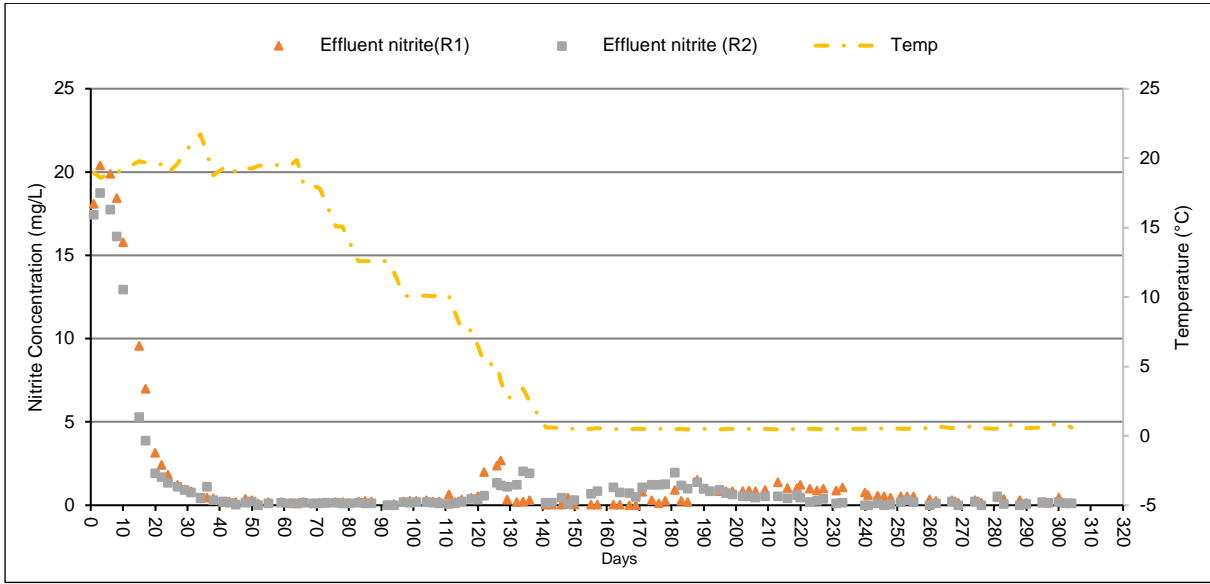


Figure 4-3 - Nitrite concentrations in R1 and R2 at temperatures from 19.5°C to 0.5°C

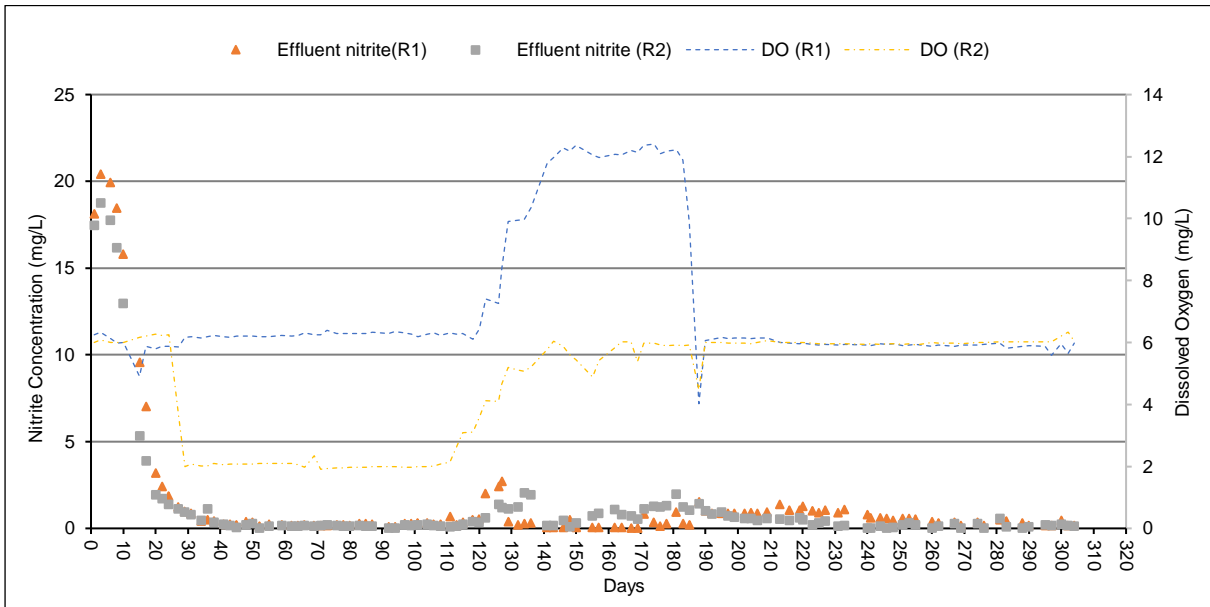


Figure 4-4 - Nitrite concentration in R1 and R2 against dissolved oxygen.

4.1.3 Nitrate Production

Upon achieving steady state in R1, complete nitrification was observed at temperatures ranging from $19.3 \pm 0.4^\circ\text{C}$ to $4.65 \pm 0.46^\circ\text{C}$ after which a rapid reduction in nitrification was observed. When operated 0.5°C there was a 47-day period with little change in nitrification followed by a gradual recovery in performance (Figure 4-5). A similar pattern was observed in R2. At $4.78 \pm 0.54^\circ\text{C}$ there was a rapid reduction in nitrate production. However, nitrate concentration remained higher in R2 for the majority of the operation 0.5°C (Figure 4-6).

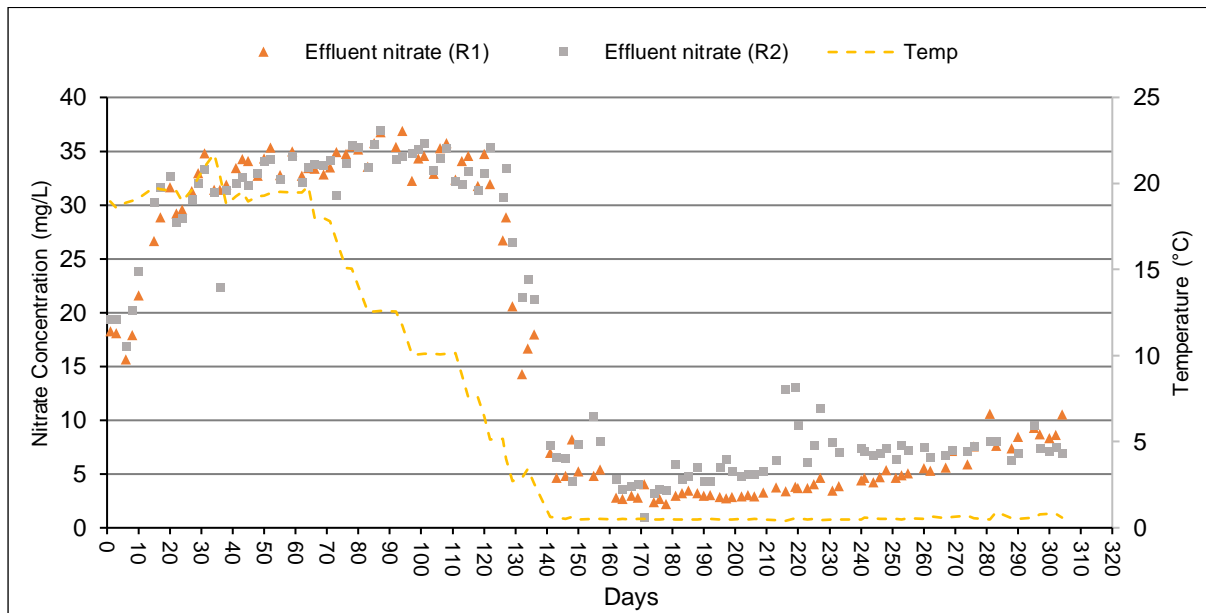


Figure 4-5 - Nitrate concentrations in R1 and R2 at temperatures from 19.5°C to 0.5°C

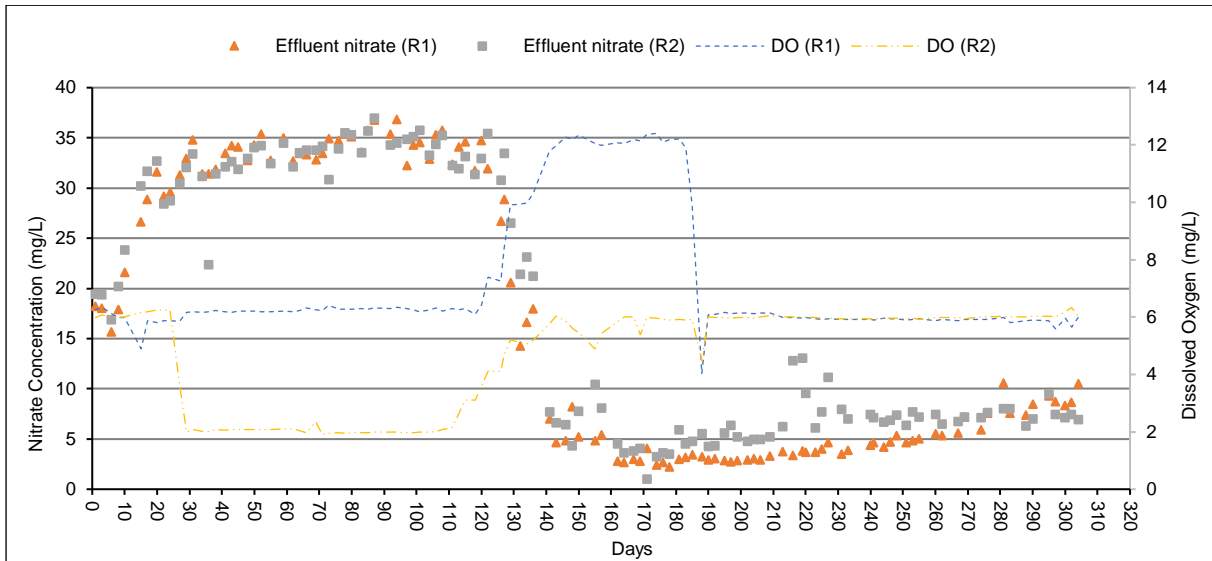


Figure 4-6 - Nitrate concentration in R1 and R2 against dissolved oxygen

4.1.4 pH and Alkalinity

In R1, the alkalinity consumption rate remained fairly constant at $2.15 \pm 0.10 \text{ g-CaCO}_3\text{m}^{-2}\text{d}^{-1}$ during operation between 19.5°C to 5°C . The alkalinity consumption rate decreased rapidly at the 5°C temperature threshold to $0.20 \pm 0.11 \text{ g-CaCO}_3\text{m}^{-2}\text{d}^{-1}$ during the stabilization and acclimatization phase at 0.5°C . During the recovery phase, there was a steady increase in consumption rate to $0.43 \text{ g-CaCO}_3\text{m}^{-2}\text{d}^{-1}$ at the end of operation at 0.5°C (Figure 4-7A). The increase in the alkalinity consumption rate at 0.5°C corresponds with the increase in ammonia oxidation.

The pH in the influent to R1 was 7.64 ± 0.18 throughout the experiment. pH in R1 remained at 7.18 ± 0.06 between 19.5°C and 2.5°C . Below 2.5°C , the pH in the reactor increased to 7.94 ± 0.22 . The higher pH in the reactor than the influent likely resulted from carbon dioxide stripping due to high aeration and low oxygen consumption below 2.5°C (Figure 4-7A).

In R2, the alkalinity consumption rate was $2.09 \pm 0.13 \text{ g-CaCO}_3\text{m}^{-2}\text{d}^{-1}$ between 19.5°C to 2.5°C . Unlike R1, the kinetic threshold in R2 was 2.5°C upon which the alkalinity rate decreased to $0.26 \pm 0.11 \text{ g-CaCO}_3\text{m}^{-2}\text{d}^{-1}$ during the stabilization and acclimatization phase at 0.5°C . During the recovery phase, there was a steady increase in consumption rate to $0.35 \text{ g-CaCO}_3 \text{ m}^{-2}\text{d}^{-1}$ at the end of operation at 0.5°C (Figure 4-8A).

The pH in the influent to R2 was maintained at 7.64 ± 0.18 throughout the experiment. pH in R1 remained at 7.18 ± 0.06 between 19.5°C and 2.5°C . Below 2.5°C the pH in the reactor increased to 7.98 ± 0.12 (Figure 4-8b). Similar to R1, the higher pH in the reactor than the influent is likely due to carbon dioxide stripping.

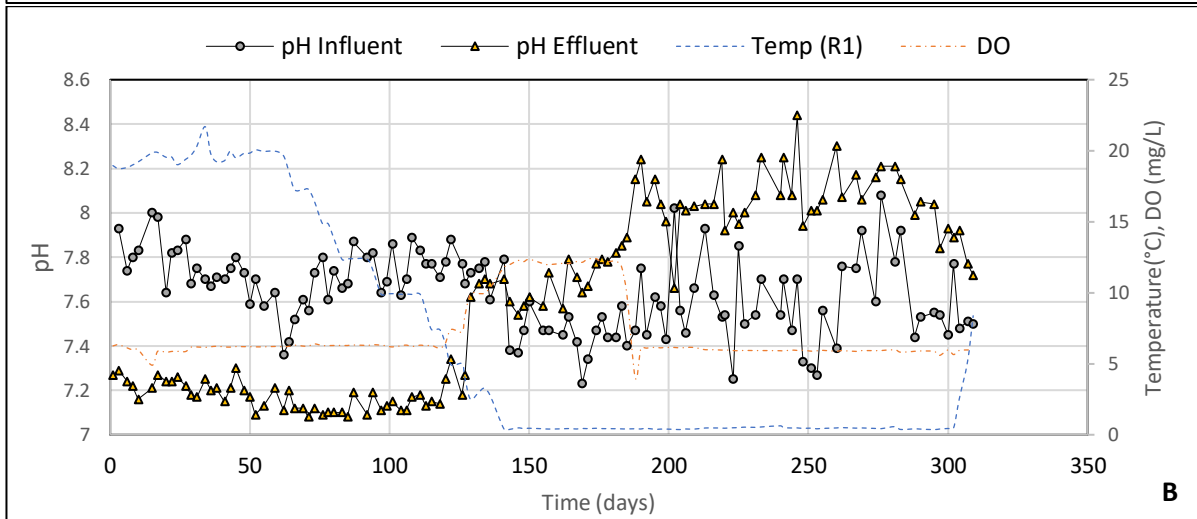
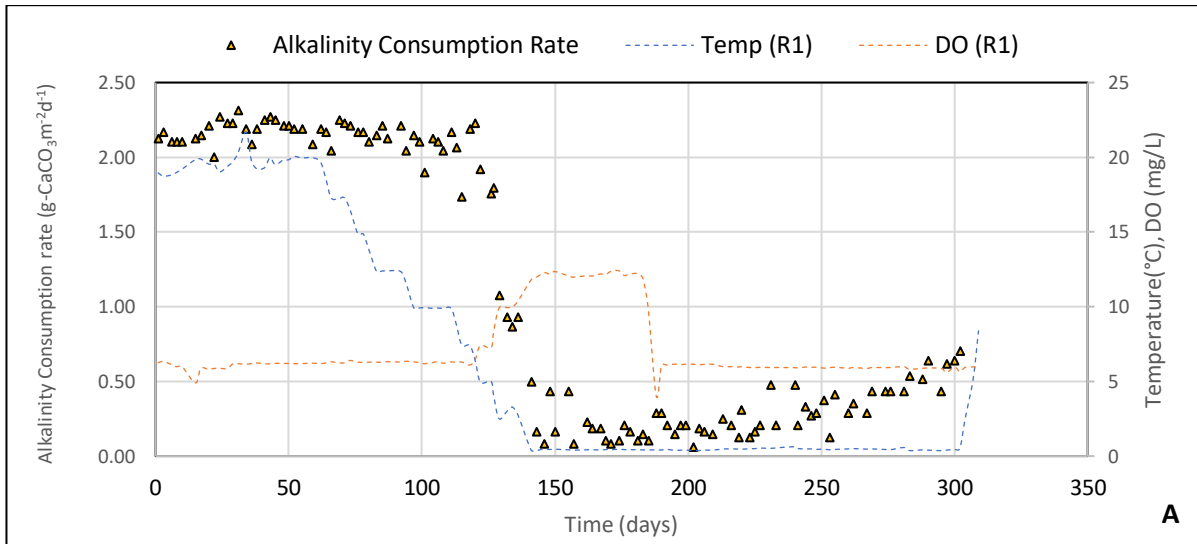


Figure 4-7 - Time-course measurements of Influent and effluent alkalinity against temperature and dissolved oxygen for R1 (A), time-course measurements of Influent and effluent pH for R1(B).

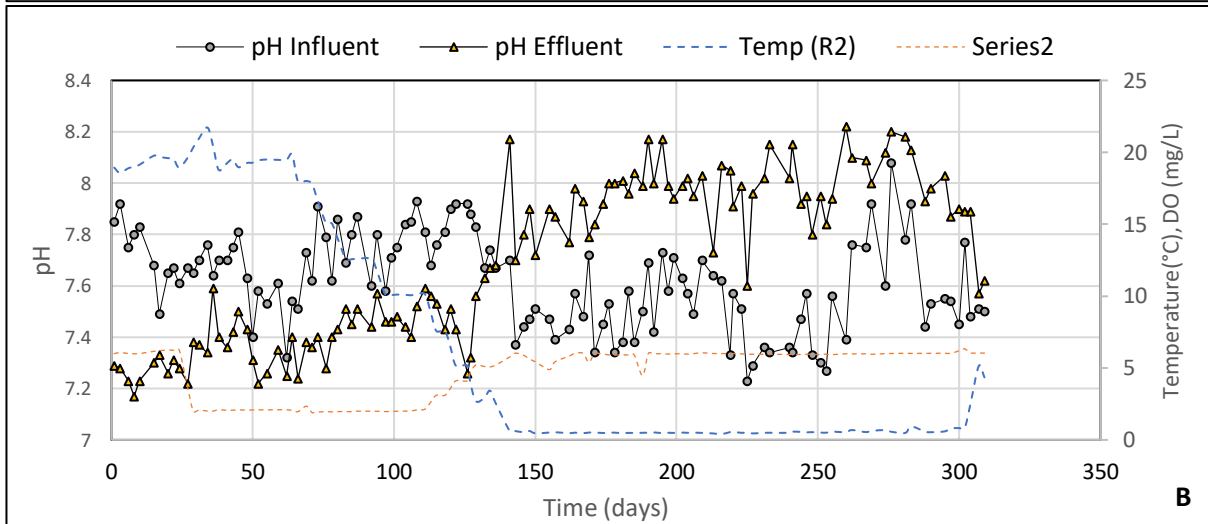
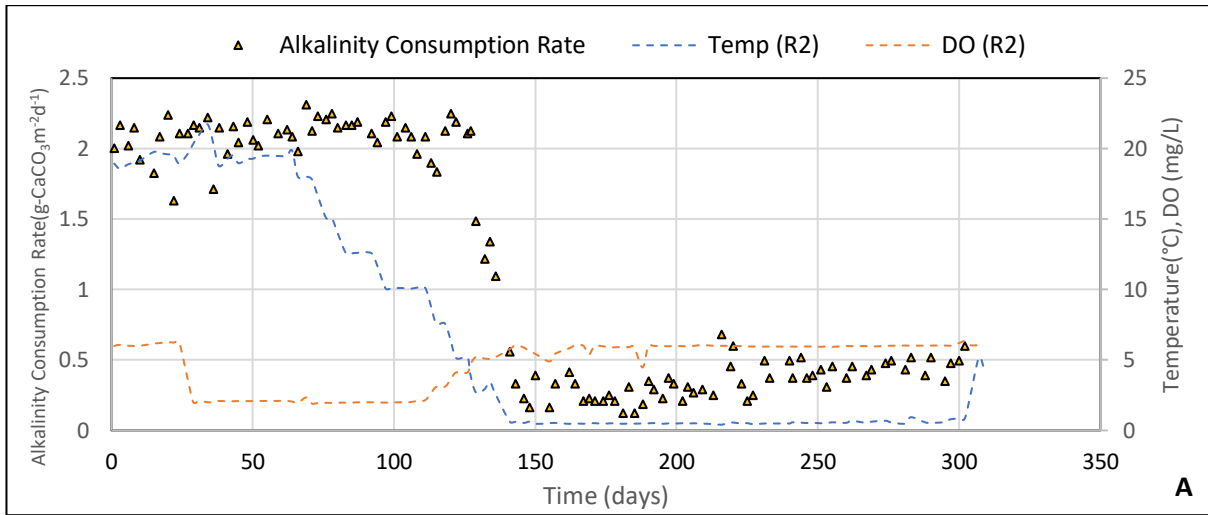


Figure 4-8 - Time-course measurements of Influent and effluent alkalinity against temperature and dissolved oxygen for R2 (A), time-course measurements of Influent and effluent pH for R2(B).

5 Chapter 5 - Discussion

5.1 Low Temperature Effect on Nitrification

Previous studies have shown sharp decreases in ammonia removal rates in MBBR systems at temperatures below 4°C [11,15,27,71–73]. Such was the case with this study where the average ammonia removal rates at 0.5°C were determined to be $0.04 \pm 0.02 \text{ g-Nm}^{-2}\text{d}^{-1}$ and $0.06 \pm 0.02 \text{ g-Nm}^{-2}\text{d}^{-1}$ in R1 and R2, respectively, which represents $15.32 \pm 8.44\%$ and $20.10 \pm 7.15\%$ of the rates at 19.5°C in R1 and R2. These results were within the realm of expectation as similar results were obtained in lab-scale studies by Hoang et al. (2014) [11] who achieved ammonia removal rates at 1°C to be of $17.2 \pm 5.1\%$ of the rates at 20°C and Ashkanami et al. (2019) who achieved 20.4% ammonia removal at 4°C relative 20°C [77]. Both of the above-mentioned studies were operated at DO concentrations greater than 4 mg/L. The results of the current study contrast significantly with those obtained at the pilot scale by Young et al. (2017) who achieved removal rates at 1°C in excess of 77% of the rates 20°C [12]. Possible reasons for the large discrepancy in the removal rates between this study and the pilot study by Young et al. (2017) could be limited temperature control as the pilot benefited from natural temperature fluctuations. Another reason could be the use of real wastewater as opposed to synthetic wastewater used in this study. Almomani et al. (2014) observed a decrease in removal rates when switching from real wastewater to synthetic wastewater [75].

The ammonia removal rates at 0.5°C were observed to stabilize in the first 27 and 22 days in R1 and R2, respectively. The long stabilization times were expected as nitrifiers have slow generation times at cold temperatures as compared with heterotrophic bacteria [78].

Delatolla et al. (2009) reported ammonia removal rates stabilizing after a two-month period in a biological aerated filter at 4°C, while Hoang et al. (2014) reported ammonia removal rates of MBBR laboratory reactors operated at 1°C stabilizing after one month [14,26]. After stabilizing R1 underwent a 37-day acclimatization period where the removal efficiency was relatively constant $10 \pm 1.1\%$. In R2 the acclimatization period was 16 days with a removal efficiency of $12 \pm 3.7\%$. While the differences in the efficiencies at 0.5°C are statistically significant ($p = 0.0007$), it is likely DO-related rather than temperature-related and is discussed in section 5.3. During the acclimatization period, both reactors experienced a spike in the nitrite concentration from 0.22 mg/L to 2.70 mg/L and 0.51 mg/L to 1.93 mg/L in R1 and R2, respectively. The nitrite concentrations gradually decreased to 0.15 mg/L and 0.12 mg/L over 81 days and 50 days in R1 and R2, respectively. These results contrast with results reported in Delatolla et al. (2009), Hoang et al. (2014) and Young et al. (2017) where spikes in nitrite concentration at 1°C were only observed during temperature shock events and were quickly oxidized to nitrate. This indicates that NOB have increased sensitivity to temperatures as low as 0.5°C. It is also possible that the inhibition of NOB at 0.5°C was as a result of free ammonia (FA) concentrations. The FA concentration was as high as 0.61 mg-N/L at pH 8.44 and 0.344 mg-N/L at pH 8.17 in R1 and R2, respectively. While these FA concentrations are below the conventional toxicity threshold for AOB inhibition, they are within the 0.1 mg-N/L – 1.0 mg-N/L threshold for NOB inhibition[3]. Studies of FA inhibition do not include data at very low temperatures. Hence, FA inhibition is likely amplified at 0.5°C, thus pH control at 0.5°C could aid nitrification.

5.1.1 Nitrification Recovery at 0.5°C

After a long acclimatization period to 0.5°C, nitrification performance in both reactors began to recover. In R1, recovery began after 64 days of operation at 0.5°C and continued for the duration of operation at 0.5°C. The recovery rate for nitrite/nitrate production in R1 was determined to be 0.11 mg-NO_xm⁻²d⁻¹. In R2, recovery began after 22 days at 0.5°C. The recovery rate in R2 was 63.5% lower than R1 at 0.04 mg-NO_xm⁻²d⁻¹ (Figure 5-1). The lower recovery rate in R2 was reflected in the nitrification batch kinetic test, where the biomass-specific nitrification rate (Section 5.5) in R2 was found to be 62% less than the rate in R1. The recovery in the reactors allowed ammonia removal rates to reach as high as 0.09 g-Nm⁻²d⁻¹ and 0.08 g-Nm⁻²d⁻¹ in R1 and R2, respectively. These respective rates represent 33.91% and 26.90% of the rates at 19.5°C. These results contrast with the results observed in previous studies [10,11,73]. Hoang et al. (2013) and Almomani et al. (2013) observed no recovery in ammonia removal performance after 120 days and 98 days of operation at 1°C, respectively, while Delatolla et al. (2009) observed a gradual decrease in performance over 95 days at 4°C. One possible reason for lack of recovery in the above-mentioned studies could be as a result of temperature shock due to the short temperature reduction schedule. Hoang et al. (2013) and Delatolla et al. (2009) reduced temperature from 20°C over 39 days and 21 days respectively, while Almomani et al. (2013) began the study at 1°C. In contrast with the above-mentioned studies, the temperature in this study was reduced from 19.5°C to 0.5°C over 120 days. As such, it is possible that the long temperature reduction schedule resulted in the bacteria experiencing shorter stabilization phases and experiencing recovery of nitrification

performance. Another possible reason for the recovery in nitrification could be an increase in live cell coverage in the biofilm over the long exposure to 0.5°C. Several studies have reported increases in the biomass viability at 1°C in nitrifying MBBR systems [27,53,76]. The increase in cell viability has been previously attributed to an increase in substrate availability throughout the biofilm as metabolic activities decrease due to low temperature [48,49]. It is likely that this also occurred in this study at 0.5°C and thus contributed to the recovery of nitrification.

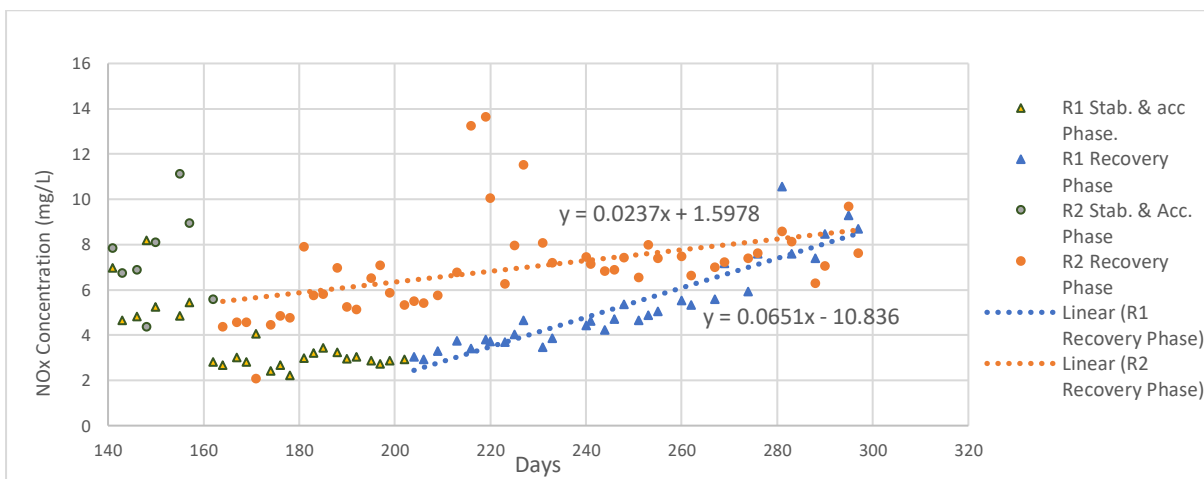


Figure 5-1- Recovery in ammonia oxidation in R1 and R2 at 0.5 degrees Celsius.

5.2 Temperature Correction Coefficient Analysis

The Arrhenius temperature correction coefficient model has been used in several studies to predict ammonia removal rates as a function of temperature change in nitrifying MBBR systems [10,15,77–79]. Typical correction coefficient values used in biofilm systems above 10°C are 1.098 and 1.058 for ammonia limiting and DO-limiting conditions, respectively [79]. Several studies have aimed to determine the temperature correction coefficient below 4°C;

however, that value has varied widely among the literature. Young et al. (2017) applied a coefficient of 1.125 to predict with strong correlation ($R^2 = 0.77$) the immediate effects of transitioning from 5°C to 1°C; after steady-state, that coefficient shifted to 1.086 [12]. Ahmed et al. (2019) applied a coefficient of 1.149 to predict removal rates between 4°C and 1°C [15].

BioWin modeling was used in this study to determine the temperature correction coefficients between 5°C and 0.5°C. Using a temperature correction coefficient of 1.15, the model was able to predict the effluent ammonia and nitrate results in R1 for the transition from 5°C to 0.5°C and the first 47 days of operation at 0.5°C with a strong correlation; R^2 being 0.92 and 0.93 for the effluent ammonia and nitrate, respectively. Beyond day 47, ammonia removal performance began to recover, resulting in R^2 falling to 0.77 for effluent ammonia and 0.02 for effluent nitrate over the remainder of operation at 0.5°C (Figure 5-2).

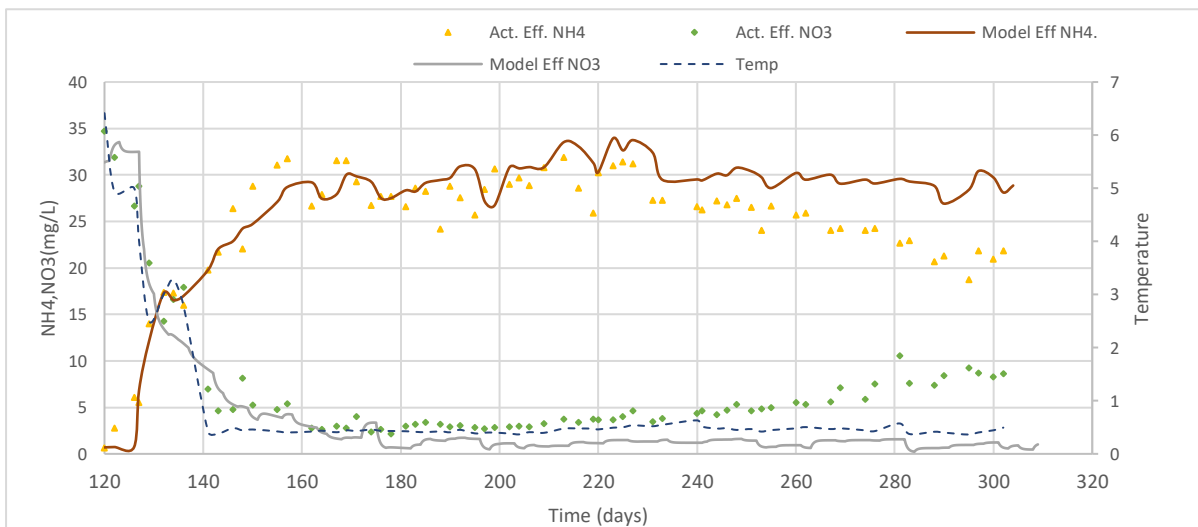


Figure 5-2 - Comparison between the effluent ammonia and nitrate predicted by the BioWin model and the experimental effluent ammonia and nitrate for the transition from 5°C to 0.5°C in R1 using a temperature correction factor of 1.15.

These results suggest that a temperature correction factor of 1.15 is able to adequately predict not only the immediate effects of transitioning to very low temperatures (0.5°C) but also the removal rates in the acclimatization phase. However, once recovery in ammonia removal begins, exposure time to 0.5°C would have to be accounted for in determining removal rates. Delatolla et al. (2009) proposed a time-dependent model for the temperature correction factor to predict the transition from 8°C to 4°C. Several studies have since applied the Delatolla et al model to simulate the transition from 4°C to 1°C with differing levels of success [11,15,27]. Young et al. (2017) and Hoang et al. (2014) found a strong correlation for the transition from 4°C to 1°C ($R^2 = 0.89$ and $R^2 = 0.86$, respectively). Ahmed et al. (2019) found a poor correlation[15]. In this study, the Delatolla et al. model was applied to factor in exposure time to 0.5°C. However, it displays a poor correlation between the modeled and experimental results (Figure 5-3). As such, it is not suitable at temperatures where recovery in removal rates is expected.

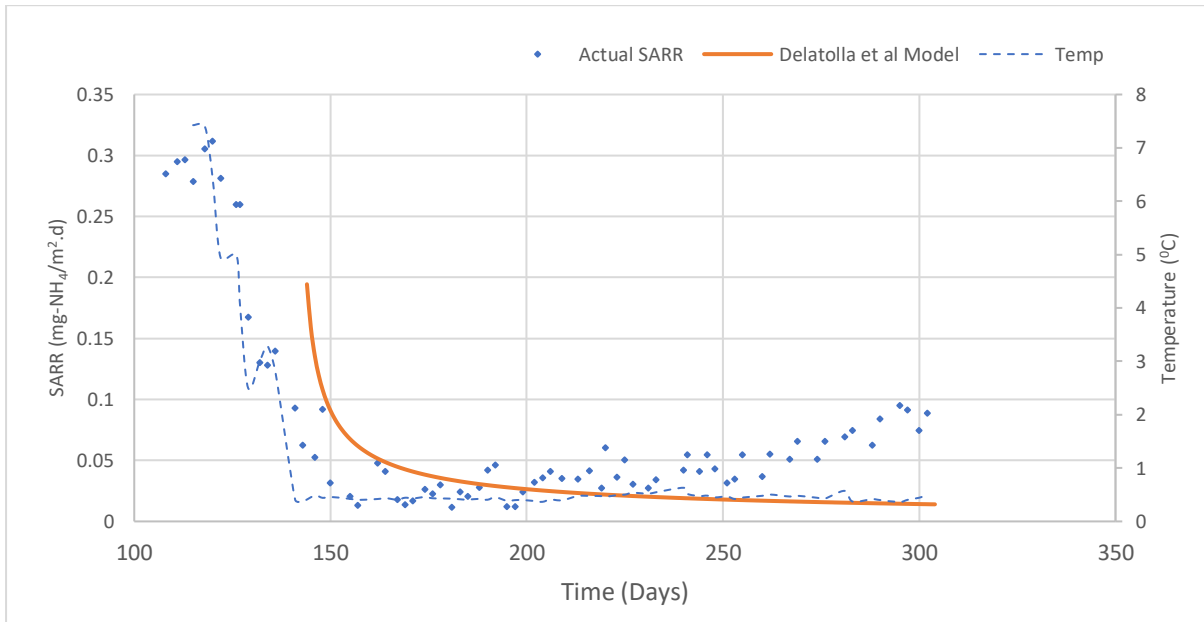


Figure 5-3 - Comparison of the ammonia removal rates predicted with Delatolla et al. (2009) model and observed experimental ammonia removal rates in R1.

5.2.1 Effect of DO Limitation on the Temperature Correction Coefficient

Several factors influence the temperature correction coefficient; factors such as the temperature range, temperature reduction schedule, and whether the nitrification reaction is ammonia limited or dissolved oxygen-limited. [70]. In this study, the nitrification reaction in R2 was DO limited between 19.5°C and 10°C. As such, it was generally expected that the nitrification rates would decrease due to low DO as well as decrease with temperature. However, the effects of low DO between 19.5°C, and 10°C were compensated for by the additional biomass which accumulated due to the reduced endogenous decay rate at long-term low DO (Section 5.3 and 5.5). This additional biomass was also able to partially compensate for the decreased metabolic activity at 0.5°C. As such, a temperature correction coefficient of 1.130 was used for R2 as opposed to 1.150 for R1. Using a temperature

correction coefficient of 1.13, the BioWin model was able to predict the effluent ammonia and effluent nitrate for the transition from 5°C to 0.5°C and the first 73 days of operation at 0.5°C with strong correlation; R^2 being 0.94 and 0.91, respectively (Figure 5-4). Similar to R1, the Delatolla et al. model showed poor correlation with the experimental results (Figure 5-5).

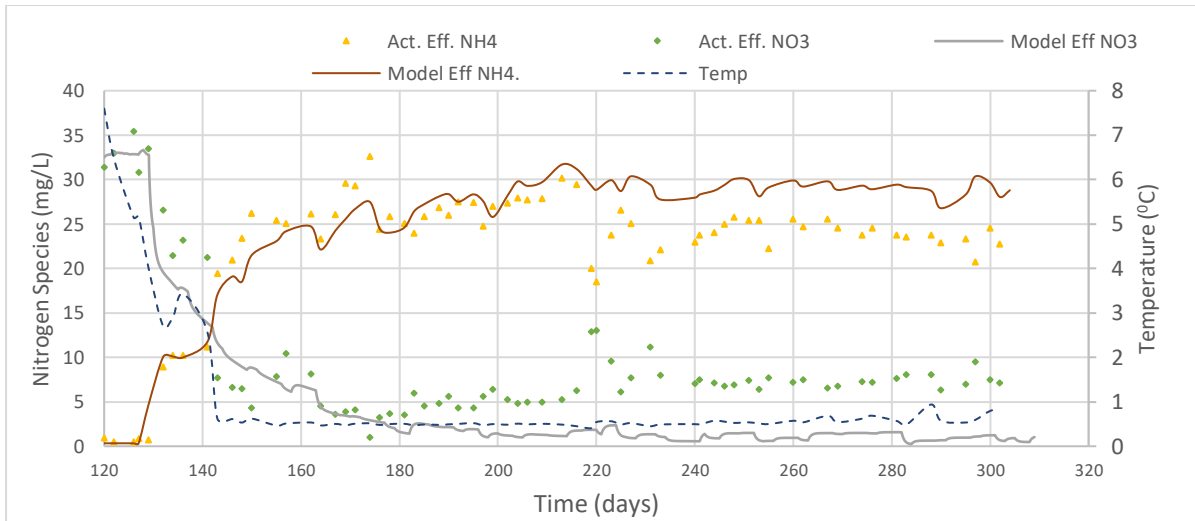


Figure 5-4 - Comparison between the effluent ammonia and nitrate predicted by BioWin model and experimental effluent ammonia and nitrate for the transition from 5°C to 0.5°C in R2 using a temperature correction factor of 1.13.

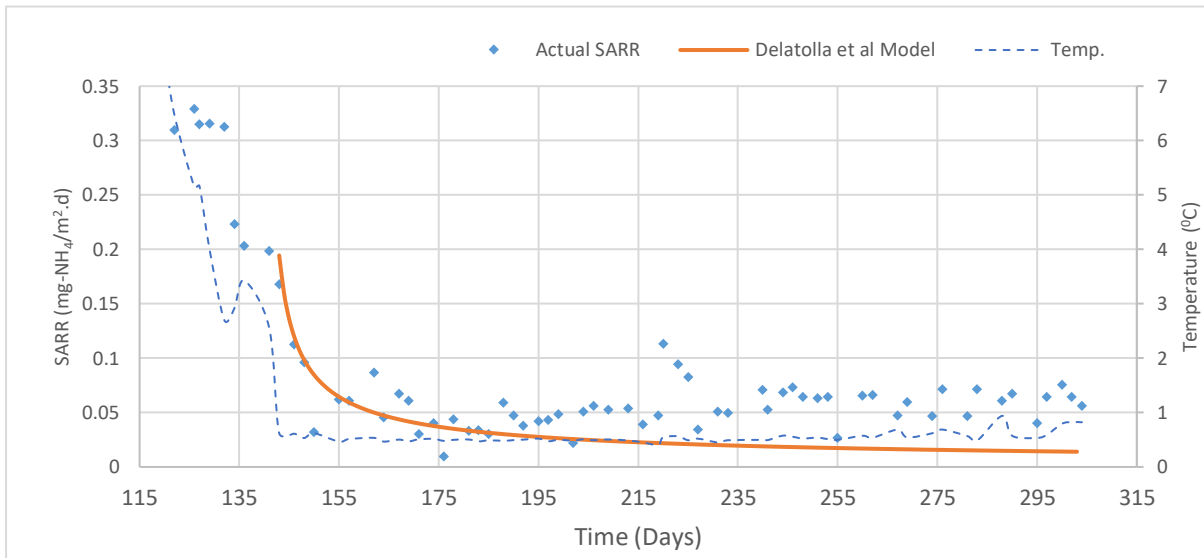


Figure 5-5 - Comparison of the ammonia removal rates predicted with Delatolla et al. (2009) model and observed experimental ammonia removal rates in R2.

5.3 DO Limitation on Nitrification

At room temperature and DO of 6mg/L, the differences in ammonia removal rates in R1 and R2 were statistically insignificant ($p = 0.17$). Upon lowering the DO to 2mg/L in R2, the differences in the removal rates between R1 and R2 showed only marginal significance ($p = 0.077$). Studies have shown that nitrification rates in biofilms increase up to bulk DO concentrations greater than 10 mg/L [82,83]; however, that is dependent on the biofilm thickness and density. The high bulk DO concentration allows for oxygen to penetrate deep into the biofilm creating a thicker active biomass layer, thus increasing the nitrification rate [84]. For this reason, it was an expectation of this study that the nitrification rates in R1 would be greater than that in R2 between 19.5°C and 10°C due to operating R2 at 2 mg/L as opposed to 6 mg/L in R1. However, the differences in the ammonia removal rates were only marginally

significant. This was likely due to the effluent ammonia concentrations being too low (< 1 mg/L) to discern the differences. It was also possible that ammonia was the limiting substance during that period. However, the effects of low DO operation were clearer when exploring the alkalinity consumption rates between the reactors where the differences showed statistical significance ($p = 0.0001$). The lower alkalinity consumption rate in R2 indicated that some DO limitation occurred. Partial nitrification and in some cases, denitrification is known to occur in biofilms under DO-limited conditions [3]. However, nitrogen mass balances in both R1 and R2 between 19.5°C and 10°C confirm nitrification as the predominant nitrogen pathway. This would indicate that though some DO limitation occurred in the biofilms at DO 2mg/L , oxygen-limited conditions were never fully established.

The temperature change between 19.5°C and 10°C was accompanied by a significant increase in the biofilm mass on the carriers in R1 and R2. Of particular note was a higher mass of biomass on the carriers in R2 than R1, which signifies that some DO limitation occurred within the biofilms in R2. The long-term operation at low DO likely inhibited the nitrifier decay rate, which resulted in greater nitrifier concentration. This may explain the insignificance ($P = 0.47$) between the ammonia removal rates in R1 and R2 between 19.5°C and 10°C . It is probable that the greater nitrifier concentration reduced the adverse effect of the low DO on the overall nitrification performance [3,34].

Below 10°C the DO concentration in R2 was increased in 1 mg/L increments for every 2.5°C reduction in temperature. The purpose of increasing the DO concentration was to ensure full penetration of the additional biofilm mass, which was expected to increase the nitrification

kinetics to compensate for the decrease in cellular activity due to the low temperature. The results of this strategy were evident at 4.65 ± 0.46 °C and 4.78 ± 0.54 °C in R1 and R2, respectively; where the removal efficiency in R1 decreased from 98% to 82% over a 7-day period. Over the same 7-day period, the removal efficiency in R2 remained at 98%. In fact, the first significant drop in removal efficiency was recorded at 2.70°C, where there was a rapid decrease to 71%. This is also supported by the greater alkalinity consumption in R2 below 10°C.

During operation at 4.65 ± 0.46 °C and 4.78 ± 0.54 °C in R1 and R2, respectively, nitrite accumulated to 2.70 mg/L in R1 and 1.36 mg/L in R2, signifying that NOB has greater sensitivity to temperature than AOB. Similar observations were made in Delatolla et al. (2009) who observed increased nitrite concentrations during temperature shocks in BAF treatment systems[26]. The higher ammonia removal rate and lower nitrite concentration in R2 indicate that nitrifier enrichment by DO limitation is able to partially compensate for lower kinetics. At 0.5°C the mass of biomass on the carriers in R2 was 20% higher than the mass of biomass on the carriers in R1. The greater amount of biomass appeared to have translated to higher removal efficiencies in R2 for the first 120 days of operation at 0.5°C.

At 0.5°C, there was an issue with DO control in R1 resulting in the DO increasing as high as 12.40 mg/L before being returned 6 mg/L. However, the spike in the DO was unlikely to have influenced the ammonia removal rates in R1 as the relatively thin biofilms (<192 µm) were likely saturated at DO concentrations below 6 mg/L.

5.4 Biofilm response

The biofilm response was characterized by the changes in biofilm mass and thickness in response to temperature and DO. The biofilm mass in both reactors was significantly higher at 12.5°C as opposed to 19.5°C. The biofilm mass increased from 1.2 ± 0.17 to 3.16 ± 0.47 mg-VSS/carrier and 1.6 ± 0.5 to 3.42 ± 0.28 mg-VSS/carrier in R1 and R2, respectively. The increase in the mass is likely as a result of a combination of reduced endogenous decay due to low temperature and increased substrate availability within the biofilm due to reduced metabolic activity. Previous studies have observed similar mass responses to temperature [27,53,76]. Between 12.5°C and 0.5°C the biofilm mass on the carriers remained stable in R2. In R1 there was a slight reduction in the biofilm mass from 3.27 ± 0.24 mg-VSS/carrier to 2.77 ± 0.15 mg-VSS/carrier (Figure 5-6). The differences in the biofilm mass between R1 and R2 at 19.5°C, 12.5°C, 10°C and 0.5°C showed statistical significance ($p = 0.021$). The higher biofilm mass in R2 is likely as a result of reduced endogenous decay due to low DO. The higher mass in R2 likely explains the higher ammonia removal rates at 0.5°C.

The biofilm thickness in both reactors indicates an increase in thickness with a decrease in temperature from 19.5°C to 10°C. At 19.5°C, the nitrifying biofilm was measured at 177.57 ± 43.86 μm and 127.94 ± 19.17 μm in R1 and R2, respectively. At 10°C the thickness increased to 191.27 ± 28.79 μm and 178 ± 15.93 μm in R1 and R2, respectively, which represents an increase of 7.2% and 28.20% in the biofilm thickness (Figure 5-7). Below 10°C the biofilm thickness was stable in R2. Unfortunately, degradation of the media prevented biofilm measurements at 0.5°C in R1. The stable biofilm thickness in R2 below 10°C could indicate

that the biofilms were fully saturated at 10°C. The stability in the biofilm may also suggest that the rate of biofilm decay and the rate of biofilm growth are similarly affected by temperature below 10°C. Increases in biofilm thickness with decreasing temperatures were also observed in Hoang et al. (2014); Young et al. (2017) and Ahmed et al. (2021) [27,48,49].

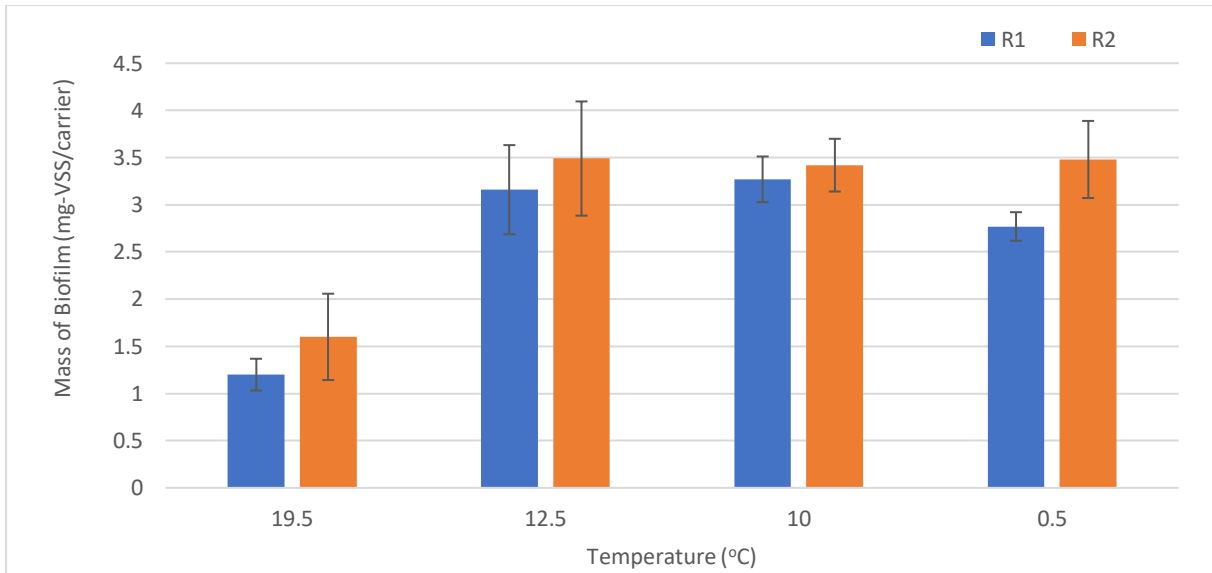


Figure 5-6 - Changes in the nitrifying biofilm mass in R1 and R2 at 19.5°C, 12.5°C, 10°C and 0.5°C.

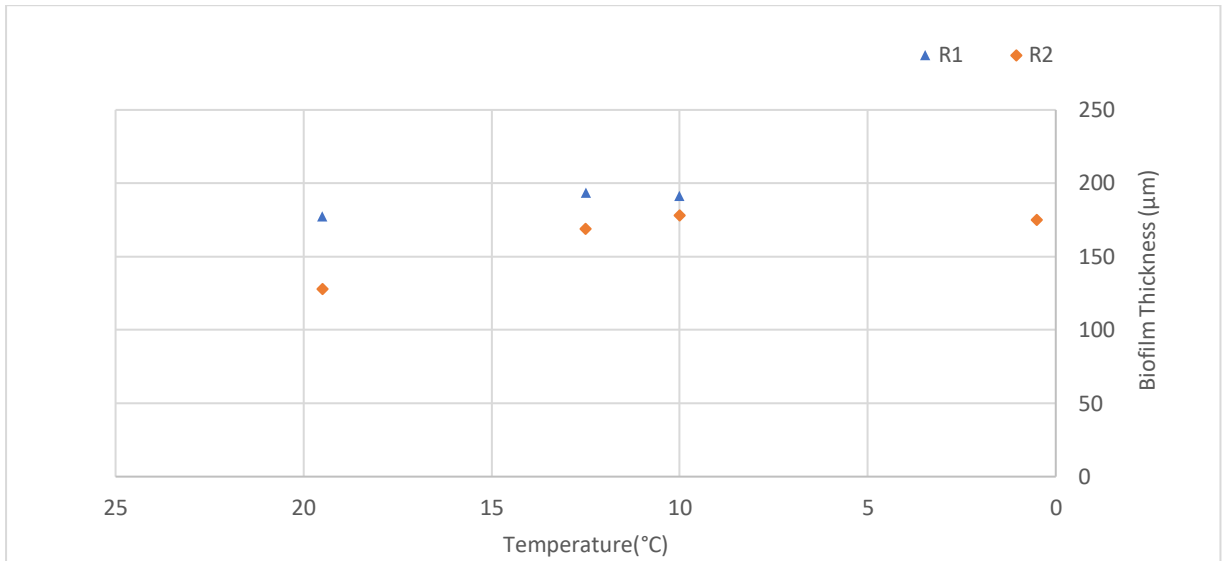


Figure 5-7 - Biofilm thickness in R1 and R2 at 19.5°C, 12.5°C, 10°C and 0.5°C.

5.5 Nitrification Batch Kinetics

Nitrification kinetic batch tests were conducted at 19.5°C, 12.5°C, 10°C, 5°C and 0.5°C to determine the biomass specific nitrification rate and the area-specific nitrification rates. It should be noted that the test at 5°C was conducted after the temperature in the reactors was increased from 0.5°C to 5°C and operated to steady-state. The results show that the difference in the biomass-specific nitrification rates between R1 and R2 has marginal significance ($p=0.065$). The higher biomass-specific nitrification rate in R1 at 19.5°C can likely be explained by the biofilm density. The biofilm thickness in R2 was 38.79% thinner than R1 despite having a higher biofilm mass, suggesting that biofilms in R2 had greater density which is known to increase substrate diffusion resistance through the biofilm matrix, thus suppressing the nitrification rate [84]. As temperature decreased, the differences in the rates were less

discernable, likely due to the decrease in metabolic activity, which allowed substrate to saturate and utilize more of the biofilm.

At 0.5°C the biomass-specific nitrification rate in R2 was 62% less than the rate in R1. The differences in the rates were evident in the ammonia removal recovery rates (Section 5.1.1). The result was unexpected as both R1 and R2 had been operated at a DO concentration greater 6 mg/L for 163 days at the time of the test. This could indicate that long-term low DO operation may have long-term effects on nitrifier growth rates. After raising the temperature to 5°C and operating to a steady state, the gap in the biomass specific rate between R1 and R2 reduced to 12%, which could indicate that re-acclimatization to high DO (>6mg/L) occurs with time. Further studies would have to be conducted to confirm this hypothesis.

The biomass-specific removal rates demonstrate a strong linear correlation, with R^2 being 0.96 and 0.92 for R1 and R2, respectively (Figure 5-8). In contrast with the biomass-specific removal rate, the area-specific removal rates show a non-linear relationship with temperature (Figure 5-9). Between 19.5°C and 10°C the removal rates remained fairly constant at 0.365 ± 0.19 g-N/m²d and decreased rapidly between 10°C and 5°C. Due to the strict temperature control schedule, batch tests between 10°C and 5°C could not be performed. However, the results of the continuous experiment demonstrated a kinetic breakpoint around 5°C. The non-linear nature of the area-specific rates despite the linear nature of the biomass-specific rates may suggest that the inherently long SRTs of biofilm technologies and the ability of biofilm technologies to accumulate biomass may contribute significantly to the temperature resistance in biofilms.

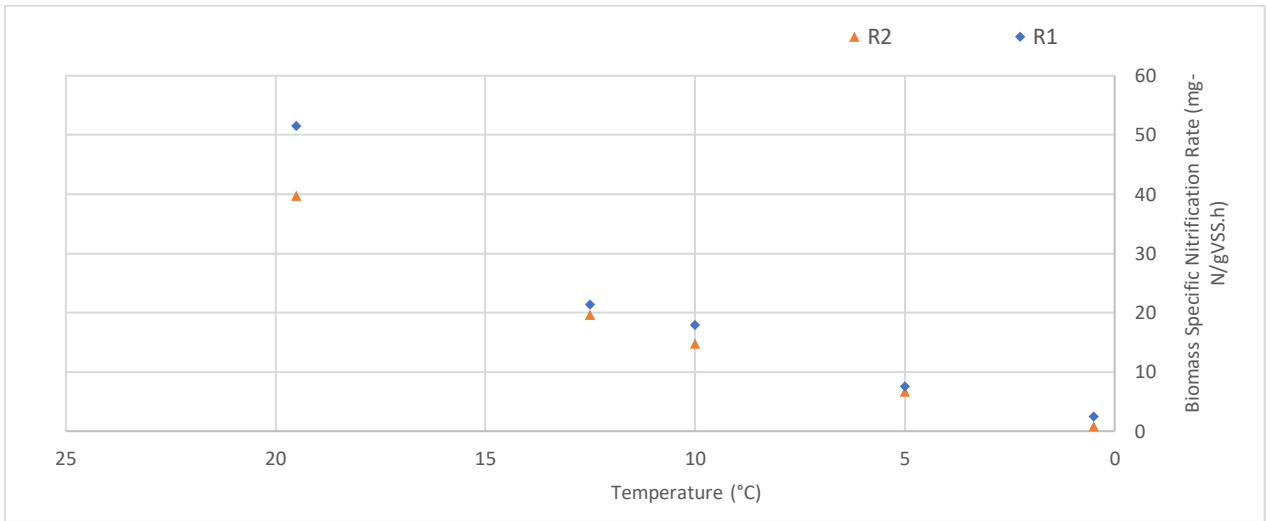


Figure 5-8 - Biomass-specific removal rates determined from the kinetic batch tests for R1 and R2 at 19.5°C, 12.5°C, 10°C and 0.5°C.

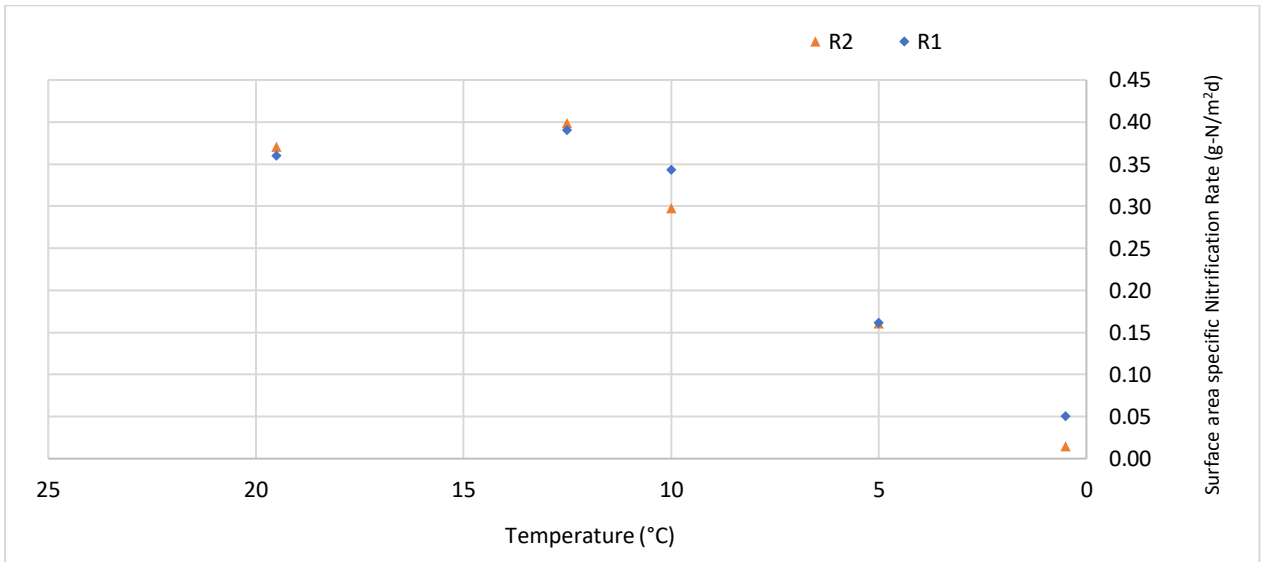


Figure 5-9 - Surface area-specific removal rates determined from the Kinetic batch tests for R1 and R2 at 19.5°C, 12.5°C, 10°C and 0.5°C.

6 Engineering Significance

Several of the observations and conclusions drawn from this research have significant impact on engineering decisions. A list of these conclusions and their significance include:

1. The differences in the ammonia removal rates between R1 (high DO) and R2 (Low DO) were insignificant from 19.5°C and 4°C despite R2 being operated at a DO concentration of 2 mg/L as opposed to 6 mg/L in R1. This conclusion has significance to design and operation as aeration accounts for more 60% of the total electricity usage for typical wastewater treatment systems [85]. Hence, significant energy savings can be realized by operating post-carbon removal nitrifying MBBR systems at 2 mg/L as opposed to the typical 6 mg/L.
2. The temperature correction coefficient was directly influenced by the biofilm mass on the carriers. This conclusion is significant as the temperature correction coefficient is an important design factor in cold temperature wastewater treatment systems and is generally accepted as being influenced by factors such as the temperature range, temperature reduction schedule, and whether the nitrification reaction is ammonia limited or dissolved oxygen-limited [79]. As such, this study shows that the expected nitrifying biofilm mass on the carriers is another factor that must be considered when selecting the temperature correction coefficient.
3. Recovery in ammonia removal occurred after long exposure to 0.5°C. This was a unique observation to this study and was likely as a result of the long temperature reduction schedule which prevented temperature shock. This observation impacts the operation of

post-carbon removal nitrifying MBBR systems as variations in the rate of temperature reduction between fall – winter temperatures will likely affect the recovery of ammonia removal at 0.5°C.

7 Summary and Conclusion

Current literature lacks studies on DO limitation to enhance nitrification at cold temperatures in nitrifying MBBR systems. This study addressed this gap in knowledge and provided new information on the optimization of the design and operation of MBBR systems to perform post-carbon ammonia removal at very cold temperatures. This was done by determining the ammonia removal rate at incremental decreases in temperature in both low DO and high DO acclimatized reactors; the kinetic threshold temperatures in both low DO and high DO acclimatized reactors; the Arrhenius temperature corrections coefficients between the kinetic breakpoint and 0.5°C and the biofilm response to temperature and DO.

This thesis study demonstrated the feasibility of applying dissolved oxygen limitation to enhance nitrification in nitrifying MBBR systems at very cold temperatures. In regards to ammonia removal efficiencies, the efficiencies between 19.5°C and 5°C in the high DO and low DO acclimatized reactors were $94.17 \pm 4.51\%$ and $93.65 \pm 6.20\%$, respectively. The differences in the efficiencies showed only marginal significance ($p = 0.077$), which indicated that cost and energy savings could be realized through long-term operation at low DO (2mg/l). Under long-term high DO, the kinetic threshold temperature was observed to be at 5°C, upon which ammonia removal rates decrease rapidly. On the other hand, under long-term low DO,

the kinetic threshold was observed at 2.5°C. Over the first 120 days at 0.5°C, the low DO acclimatized reactor proved capable of achieving higher ammonia removal efficiencies at $17.4 \pm 6.87\%$ than the high DO acclimatized reactor at $10.93 \pm 6.00\%$. In contrast with previous studies, both the low and high DO acclimatized reactors were capable of recovering nitrification performance after acclimatization to 0.5°C. Despite having lower initial removal rates, the high DO reactor recovered at $0.11 \text{ mg-NO}_x/\text{m}^2 \cdot \text{d}$ as opposed to $0.04 \text{ mg-NO}_x/\text{m}^2 \cdot \text{d}$ in the low DO reactor, which resulted in similar removal rates towards the end of the operation at 0.5°C. The recovery rates are reflected in the specific nitrification rates at 0.5°C.

The biofilms in the high and low DO reactors showed similar responses to temperature but had distinctly different responses to DO. The biofilm mass in both reactors was higher during operation at 12.5°C than 19.5°C, but relatively stable below 12.5°C. On the other hand, the biofilm mass in the low DO reactor was consistently greater than the biofilm mass in the high DO reactor which confirms the hypothesis of the study that long-term low DO is able to inhibit nitrifier endogenous decay and thus result in nitrifier enrichment in the biofilm. Additionally, the higher removal rates in the low DO acclimatized reactor despite lower biomass specific rates indicated the significance of accumulating biofilm mass prior to operation at 0.5°C.

In this study, an Arrhenius correction coefficient of 1.150 was found for the transition from 5°C to 0.5°C for nitrifying MBBR systems acclimatized to high DO. A second coefficient of 1.13 was found for the transition from 5°C to 0.5°C in low DO acclimatized nitrifying MBBR systems to account for the higher removal rates at 0.5°C. This indicated that the biofilm mass on the carriers directly influenced the Arrhenius correction coefficient.

This study demonstrates the significance of biofilm mass to performing nitrification at 0.5°C. Hence, future work should explore additional methods of accumulating nitrifying biomass prior to operation at very cold temperatures. While accumulating thick biofilms may lead to diffusion limitations at warm temperatures, the decreased metabolic activity in the biofilm at 0.5°C will allow for substrate to penetrate deeper into the biofilm, which will result in utilization of greater portions of the biofilm, thus enhancing nitrification.

8 References

- [1] C. Gazette, Wastewater Systems Effluent Regulations, (2012).
- [2] G.W. Holcombe, R.W. Andrew, The Acute Toxicity of Zinc to Rainbow and Brook Trout: Comparisons in Hard and Soft Water, *Epa-600. 3-78-094* (1978) 16.
- [3] W. Metcalf, C. Eddy, *Wastewater Engineering: Treatment and Resource Recovery*, Fifth Edition, 2014.
- [4] T.J. Hurse, M.A. Connor, Nitrogen removal from wastewater treatment lagoons, in: *Water Sci. Technol.*, 1999. [https://doi.org/10.1016/S0273-1223\(99\)00139-0](https://doi.org/10.1016/S0273-1223(99)00139-0).
- [5] J.A. Oleszkiewicz, S.A. Berquist, Low temperature nitrogen removal in sequencing batch reactors, *Water Res.* (1988). [https://doi.org/10.1016/0043-1354\(88\)90012-7](https://doi.org/10.1016/0043-1354(88)90012-7).
- [6] M.A. Head, J.A. Oleszkiewicz, Bioaugmentation for nitrification at cold temperatures, *Water Res.* (2004). <https://doi.org/10.1016/j.watres.2003.11.003>.
- [7] S.-Y. Leu, R.W. Babcock., M.K. Stenstrom, Evaluation of Bioaugmentation to Improve Wastewater Treatment, *Proc. Water Environ. Fed.* (2012). <https://doi.org/10.2175/193864709793955618>.
- [8] F. Stenström, J. La Cour Jansen, Promotion of nitrifiers through side-stream bioaugmentation: A full-scale study, *Water Sci. Technol.* (2016). <https://doi.org/10.2166/wst.2016.340>.
- [9] G. Liu, J. Wang, Long-term low DO enriches and shifts nitrifier community in activated

- sludge, Environ. Sci. Technol. 47 (2013) 5109–5117.
<https://doi.org/10.1021/es304647y>.
- [10] F.A. Almomani, R. Delatolla, B. Örmeci, Field study of moving bed biofilm reactor technology for post-treatment of wastewater lagoon effluent at 1°C, Environ. Technol. (United Kingdom). (2014). <https://doi.org/10.1080/09593330.2013.874500>.
- [11] V. Hoang, MBBR ammonia removal: an investigation of nitrification kinetics, biofilm and biomass response, and bacterial population shifts during long-term cold temperature exposure, Univ. Ottawa. (2013).
- [12] B. Young, R. Delatolla, B. Ren, K. Kennedy, E. Laflamme, A. Stintzi, Pilot-scale tertiary MBBR nitrification at 1°C: characterization of ammonia removal rate, solids settleability and biofilm characteristics, Environ. Technol. (United Kingdom). (2016). <https://doi.org/10.1080/09593330.2016.1143037>.
- [13] W. Ahmed, Nitrifying Moving Bed Biofilm Reactors at Low Temperatures and Cold Shock Conditions : A Kinetic , Biofilm and Microbiome Study, (2020).
- [14] V. Hoang, R. Delatolla, E. Laflamme, A. Gadbois, An Investigation of Moving Bed Biofilm Reactor Nitrification during Long-Term Exposure to Cold Temperatures, Water Environ. Res. 86 (2014) 36–42. <https://doi.org/10.2175/106143013x13807328848694>.
- [15] W. Ahmed, X. Tian, R. Delatolla, Nitrifying moving bed biofilm reactor: Performance at low temperatures and response to cold-shock, Chemosphere. 229 (2019) 295–302. <https://doi.org/10.1016/j.chemosphere.2019.04.176>.

- [16] G. Liu, J. Wang, Modeling effects of DO and SRT on activated sludge decay and production, *Water Res.* 80 (2015) 169–178. <https://doi.org/10.1016/j.watres.2015.04.042>.
- [17] D.P. Kelly, Autotrophy: concepts of lithotrophic bacteria and their organic metabolism., *Annu. Rev. Microbiol.* (1971). <https://doi.org/10.1146/annurev.mi.25.100171.001141>.
- [18] A.C. van Haandel, G.A. Ekama, G. v. R. Marais, The activated sludge process-3 single sludge denitrification, *Water Res.* (1981). [https://doi.org/10.1016/0043-1354\(81\)90089-0](https://doi.org/10.1016/0043-1354(81)90089-0).
- [19] B. Sharma, R.C. Ahlert, Nitrification and nitrogen removal, *Water Res.* (1977). [https://doi.org/10.1016/0043-1354\(77\)90078-1](https://doi.org/10.1016/0043-1354(77)90078-1).
- [20] R.H. Wijffels, C.D. de Gooijer, S. Kortekaas, J. Tramper, Growth and substrate consumption of *Nitrobacter agilis* cells immobilized in carrageenan: Part 2. Model evaluation, *Biotechnol. Bioeng.* (1991). <https://doi.org/10.1002/bit.260380304>.
- [21] Y.Q. Liu, G.H. Lan, P. Zeng, Resistance and resilience of nitrifying bacteria in aerobic granules to pH shock, *Lett. Appl. Microbiol.* (2015). <https://doi.org/10.1111/lam.12433>.
- [22] C. Elmerich, Nitrification and denitrification in the activated sludge process, *Res. Microbiol.* (2002). [https://doi.org/10.1016/s0923-2508\(02\)01315-3](https://doi.org/10.1016/s0923-2508(02)01315-3).
- [23] R. Margesin, G. Feller, Biotechnological applications of psychrophiles, *Environ. Technol.*

- (2010). <https://doi.org/10.1080/09593331003663328>.
- [24] W.E. Federation, Water Environment Federation, Design of Municipal Wastewater Treatment Plants, 2009.
- [25] J.H. Hwang, J.A. Oleszkiewicz, Effect of Cold-Temperature Shock on Nitrification, Water Environ. Res. (2007). <https://doi.org/10.2175/106143007x176022>.
- [26] R. Delatolla, N. Tufenkji, Y. Comeau, A. Gadbois, D. Lamarre, D. Berk, Kinetic analysis of attached growth nitrification in cold climates, Water Sci. Technol. (2009). <https://doi.org/10.2166/wst.2009.419>.
- [27] B. Young, R. Delatolla, K. Kennedy, E. Laflamme, A. Stintzi, Low temperature MBBR nitrification: Microbiome analysis, Water Res. (2017). <https://doi.org/10.1016/j.watres.2016.12.050>.
- [28] R. Delatolla, N. Tufenkji, Y. Comeau, A. Gadbois, D. Lamarre, D. Berk, Investigation of Laboratory-Scale and Pilot-Scale Attached Growth Ammonia Removal Kinetics at Cold Temperature and Low Influent Carbon, Water Qual. Res. J. (2010). <https://doi.org/10.2166/wqrj.2010.042>.
- [29] G. KNOWLES, A.L. DOWNING, M.J. BARRETT, Determination of Kinetic Constants for Nitrifying Bacteria in Mixed Culture, with the Aid of an Electronic Computer, J. Gen. Microbiol. (1965). <https://doi.org/10.1099/00221287-38-2-263>.
- [30] S. Chen, J. Ling, J.P. Blancheton, Nitrification kinetics of biofilm as affected by water

- quality factors, *Aquac. Eng.* (2006). <https://doi.org/10.1016/j.aquaeng.2005.09.004>.
- [31] S. Zhu, S. Chen, The impact of temperature on nitrification rate in fixed film biofilters, *Aquac. Eng.* (2002). [https://doi.org/10.1016/S0144-8609\(02\)00022-5](https://doi.org/10.1016/S0144-8609(02)00022-5).
- [32] T.C. Zhang, Y.-C. Fu, P.L. Bishop, Competition for substrate and space in biofilms, *Water Environ. Res.* (1995). <https://doi.org/10.2175/106143095x133220>.
- [33] K. Hanaki, C. Wantawin, S. Ohgaki, Nitrification at low levels of dissolved oxygen with and without organic loading in a suspended-growth reactor, *Water Res.* (1990). [https://doi.org/10.1016/0043-1354\(90\)90004-P](https://doi.org/10.1016/0043-1354(90)90004-P).
- [34] G. Liu, J. Wang, Long-term low DO enriches and shifts nitrifier community in activated sludge, *Environ. Sci. Technol.* (2013). <https://doi.org/10.1021/es304647y>.
- [35] G. Liu, J. Wang, Modeling effects of DO and SRT on activated sludge decay and production, *Water Res.* (2015). <https://doi.org/10.1016/j.watres.2015.04.042>.
- [36] G. Munz, C. Lubello, J.A. Oleszkiewicz, Modeling the decay of ammonium oxidizing bacteria, *Water Res.* (2011). <https://doi.org/10.1016/j.watres.2010.09.022>.
- [37] K. Hanaki, C. Wantawin, S. Ohgaki, Effects of the activity of heterotrophs on nitrification in a suspended-growth reactor, *Water Res.* (1990). [https://doi.org/10.1016/0043-1354\(90\)90003-O](https://doi.org/10.1016/0043-1354(90)90003-O).
- [38] J. Carrera, T. Vicent, J. Lafuente, Effect of influent COD/N ratio on biological nitrogen removal (BNR) from high-strength ammonium industrial wastewater, *Process Biochem.*

- (2004). <https://doi.org/10.1016/j.procbio.2003.10.005>.
- [39] K. Hanaki, C. Wantawin, S. Ohgaki, Nitrification at low levels of dissolved oxygen with and without organic loading in a suspended-growth reactor, *Water Res.* 24 (1990) 297–302. [https://doi.org/10.1016/0043-1354\(90\)90004-P](https://doi.org/10.1016/0043-1354(90)90004-P).
- [40] A. Ohashi, D.G. Viraj de Silva, B. Mobarry, J.A. Manem, D.A. Stahl, B.E. Rittmann, Influence of substrate C/N ratio on the structure of multi-species biofilms consisting of nitrifiers and heterotrophs, *Water Sci. Technol.* (1995). [https://doi.org/10.1016/0273-1223\(96\)00010-8](https://doi.org/10.1016/0273-1223(96)00010-8).
- [41] S. Navada, M.F. Knutsen, I. Bakke, O. Vadstein, Nitrifying biofilms deprived of organic carbon show higher functional resilience to increases in carbon supply, *Sci. Rep.* (2020). <https://doi.org/10.1038/s41598-020-64027-y>.
- [42] R. Vasudevan, Biofilms: Microbial Cities of Scientific Significance, *J. Microbiol. Exp.* (2014). <https://doi.org/10.15406/jmen.2014.01.00014>.
- [43] T.R. Garrett, M. Bhakoo, Z. Zhang, Bacterial adhesion and biofilms on surfaces, *Prog. Nat. Sci.* (2008). <https://doi.org/10.1016/j.pnsc.2008.04.001>.
- [44] C.S. Butler, J.P. Boltz, Biofilm Processes and Control in Water and Wastewater Treatment, in: *Compr. Water Qual. Purif.*, 2014. <https://doi.org/10.1016/B978-0-12-382182-9.00083-9>.
- [45] T.R. Garrett, M. Bhakoo, Z. Zhang, Bacterial adhesion and biofilms on surfaces, *Prog.*

- Nat. Sci. 18 (2008) 1049–1056. <https://doi.org/10.1016/j.pnsc.2008.04.001>.
- [46] L. Hall-Stoodley, P. Stoodley, Developmental regulation of microbial biofilms, *Curr. Opin. Biotechnol.* (2002). [https://doi.org/10.1016/S0958-1669\(02\)00318-X](https://doi.org/10.1016/S0958-1669(02)00318-X).
- [47] K.Y. Le, S. Dastgheyb, T. V. Ho, M. Otto, Molecular determinants of staphylococcal biofilm dispersal and structuring, *Front. Cell. Infect. Microbiol.* (2014). <https://doi.org/10.3389/fcimb.2014.00167>.
- [48] V. Hoang, R. Delatolla, T. Abujamel, W. Mottawea, A. Gadbois, E. Laflamme, A. Stintzi, Nitrifying moving bed biofilm reactor (MBBR) biofilm and biomass response to long term exposure to 1°C, *Water Res.* (2014). <https://doi.org/10.1016/j.watres.2013.11.018>.
- [49] W. Ahmed, R. Delatolla, Biofilm and microbiome response of attached growth nitrification systems across incremental decreases to low temperatures, *J. Water Process Eng.* 39 (2021).
- [50] R.O. Mines, J.H. Sherrard, Temperature interactions in the activated sludge process, *J. Environ. Sci. Heal. - Part A Toxic/Hazardous Subst. Environ. Eng.* (1999). <https://doi.org/10.1080/10934529909376839>.
- [51] W. Dunne, Michael, Bacterial Adhesion: Seen Any Good Biofilms Lately?, *Clin. Microbiol. Rev.* (2002) 155–166. <https://doi.org/10.1128/CMR.15.2.155-166.2002>.
- [52] E. Loupasaki, E. Diamadopoulos, Attached growth systems for wastewater treatment

- in small and rural communities: A review, *J. Chem. Technol. Biotechnol.* (2013).
<https://doi.org/10.1002/jctb.3967>.
- [53] E.J.T.M. Leenen, A.M.G.A. Van Boxtel, G. Englund, J. Tramper, R.H. Wijffels, Reduced temperature sensitivity of immobilized *Nitrobacter agilis* cells caused by diffusion limitation, *Enzyme Microb. Technol.* (1997). [https://doi.org/10.1016/S0141-0229\(96\)00214-1](https://doi.org/10.1016/S0141-0229(96)00214-1).
- [54] A. Kapoor, A. Kuiper, P. Bedard, W.D. Gould, Use of a rotating biological contactor for removal of ammonium from mining effluents, *Eur. J. Miner. Process. Environ. Prot.* (2003).
- [55] L. Mendoza-Espinosa, T. Stephenson, A review of biological aerated filters (BAFs) for wastewater treatment, *Environ. Eng. Sci.* (1999).
<https://doi.org/10.1089/ees.1999.16.201>.
- [56] R.D. Miller, J.A. Hittlebaugh, C.I. Noss, E.D. Smith, NITRIFICATION USING THE ROTATING BIOLOGICAL CONTACTOR., in: *AIChE Symp. Ser.*, 1981.
- [57] H. Ødegaard, Innovations in wastewater treatment: The moving bed biofilm process, *Water Sci. Technol.* (2006). <https://doi.org/10.2166/wst.2006.284>.
- [58] D.W. Han, H.J. Yun, D.J. Kim, Autotrophic nitrification and denitrification characteristics of an upflow biological aerated filter, *J. Chem. Technol. Biotechnol.* (2001).
<https://doi.org/10.1002/jctb.499>.

- [59] J.A. Oleszkiewicz, J.L. Barnard, Nutrient removal technology in North America and the European Union: A review, *Water Qual. Res. J. Canada*. (2006). <https://doi.org/10.2166/wqrj.2006.048>.
- [60] S.. Reed, C.. Diener, P.B. Weyrick, Nitrogen removal in cold regions trickling filter systems, Hanover, New Hampshire, 1987.
- [61] G.P. Ltd, *Trickling Filter Technology for Treating Abattoir Wastewater*, 2015.
- [62] T. Wik, Trickling filters and biofilm reactor modelling, *Rev. Environ. Sci. Biotechnol.* (2003). <https://doi.org/10.1023/B:RESB.0000040470.48460.bb>.
- [63] M.M.-G. Saidu, Temperature Impact on Nitrification and Bacterial Growth Kinetics in Acclimating Recirculating Aquaculture Systems Biofilters, *Engineering*. (2009).
- [64] B. Wortman, F. Wheaton, Temperature effects on biodrum nitrification, *Aquac. Eng.* (1991). [https://doi.org/10.1016/0144-8609\(91\)90023-D](https://doi.org/10.1016/0144-8609(91)90023-D).
- [65] S. Cortez, P. Teixeira, R. Oliveira, M. Mota, Rotating biological contactors: A review on main factors affecting performance, *Rev. Environ. Sci. Biotechnol.* (2008). <https://doi.org/10.1007/s11157-008-9127-x>.
- [66] O. Nowak, Upgrading of wastewater treatment plants equipped with rotating biological contactors to nitrification and P removal, *Water Sci. Technol.* (2000). <https://doi.org/10.2166/wst.2000.0023>.
- [67] G. Farabegoli, A. Chiavola, E. Rolle, The Biological Aerated Filter (BAF) as alternative

- treatment for domestic sewage. Optimization of plant performance, *J. Hazard. Mater.* (2009). <https://doi.org/10.1016/j.jhazmat.2009.06.128>.
- [68] J.H. Ha, S.K. Ong, R. Surampalli, J. Song, Temperature effects on nitrification in polishing biological aerated filters (BAFs), *Environ. Technol.* (2010). <https://doi.org/10.1080/09593331003610915>.
- [69] A. di Biase, M.S. Kowalski, T.R. Devlin, J.A. Oleszkiewicz, Moving bed biofilm reactor technology in municipal wastewater treatment: A review, *J. Environ. Manage.* (2019). <https://doi.org/10.1016/j.jenvman.2019.06.053>.
- [70] R. Salvetti, A. Azzellino, R. Canziani, L. Bonomo, Effects of temperature on tertiary nitrification in moving-bed biofilm reactors, *Water Res.* (2006). <https://doi.org/10.1016/j.watres.2006.05.013>.
- [71] G. Andreottola, P. Foladori, M. Ragazzi, Upgrading of a small wastewater treatment plant in a cold climate region using a moving bed biofilm reactor (MBBR) system, *Water Sci. Technol.* (2000). <https://doi.org/10.2166/wst.2000.0027>.
- [72] A. di Biase, T.R. Devlin, J.A. Oleszkiewicz, Start-Up of an Anaerobic Moving Bed–Biofilm Reactor and Transition to Brewery Wastewater Treatment, *J. Environ. Eng.* (2016). [https://doi.org/10.1061/\(asce\)ee.1943-7870.0001146](https://doi.org/10.1061/(asce)ee.1943-7870.0001146).
- [73] APHA, AWWA, WEF, *Standard Methods for Examination of Water and Wastewater*, Washingt. Am. Public Heal. Assoc. (2012).

- [74] M. Piculell, P. Welander, K. Jönsson, T. Welander, Evaluating the effect of biofilm thickness on nitrification in moving bed biofilm reactors, *Environ. Technol.* (United Kingdom). (2016). <https://doi.org/10.1080/09593330.2015.1080308>.
- [75] F.A. Almomani, R. Delatolla, B. Örmeci, Field study of moving bed biofilm reactor technology for post-treatment of wastewater lagoon effluent at 1°C, *Environ. Technol.* (United Kingdom). 35 (2014) 1596–1604. <https://doi.org/10.1080/09593330.2013.874500>.
- [76] R. Delatolla, N. Tufenkji, Y. Comeau, A. Gadbois, D. Lamarre, D. Berk, Effects of Long Exposure to Low Temperatures on Nitrifying Biofilm and Biomass in Wastewater Treatment, *Water Environ. Res.* (2012). <https://doi.org/10.2175/106143012x13354606450924>.
- [77] A. Ashkanani, F. Almomani, M. Khraisheh, R. Bhosale, M. Tawalbeh, K. AlJaml, Bio-carrier and operating temperature effect on ammonia removal from secondary wastewater effluents using moving bed biofilm reactor (MBBR), *Sci. Total Environ.* (2019). <https://doi.org/10.1016/j.scitotenv.2019.07.231>.
- [78] R.H. Wijffels, J.H. Hunik, E.J.T.M. Leenen, A. Günther, J.M.O. de Castro, J. Tramper, G. Englund, Bakketun, Effects of diffusion limitation on immobilized nitrifying microorganisms at low temperatures, *Biotechnol. Bioeng.* (1995). <https://doi.org/10.1002/bit.260450102>.
- [79] R. Salvetti, A. Azzellino, R. Canziani, L. Bonomo, Effects of temperature on tertiary

- nitrification in moving-bed biofilm reactors, *Water Res.* 40 (2006) 2981–2993.
<https://doi.org/10.1016/j.watres.2006.05.013>.
- [80] R. Delatolla, N. Tufenkji, Y. Comeau, A. Gadbois, D. Lamarre, D. Berk, Investigation of Laboratory-Scale and Pilot-Scale Attached Growth Ammonia Removal Kinetics at Cold Temperature and Low Influent Carbon, *Water Qual. Res. J.* 45 (2010) 427–436.
<https://doi.org/10.2166/wqrj.2010.042>.
- [81] V. Hoang, R. Delatolla, E. Laflamme, A. Gadbois, An Investigation of Moving Bed Biofilm Reactor Nitrification during Long-Term Exposure to Cold Temperatures, *Water Environ. Res.* (2014). <https://doi.org/10.2175/106143013x13807328848694>.
- [82] D.J. Gapes, J. Keller, Impact of oxygen mass transfer on nitrification reactions in suspended carrier reactor biofilms, *Process Biochem.* (2009).
<https://doi.org/10.1016/j.procbio.2008.09.004>.
- [83] H. Odegaard, B. Rusten, T. Westrum, A new moving bed biofilm reactor - applications and results, in: *Water Sci. Technol.*, 1994. <https://doi.org/10.2166/wst.1994.0757>.
- [84] M. Piculell, P. Welander, K. Jönsson, T. Welander, Evaluating the effect of biofilm thickness on nitrification in moving bed biofilm reactors, *Environ. Technol. (United Kingdom)*. 37 (2016) 732–743. <https://doi.org/10.1080/09593330.2015.1080308>.
- [85] J. Sun, P. Liang, X. Yan, K. Zuo, K. Xiao, J. Xia, Y. Qiu, Q. Wu, S. Wu, X. Huang, M. Qi, X. Wen, Reducing aeration energy consumption in a large-scale membrane bioreactor: Process simulation and engineering application, *Water Res.* (2016).

<https://doi.org/10.1016/j.watres.2016.02.026>.